Available online at www.sciencedirect.com
SCIENCE DIRECT®
Coordination Chemistry Reviews 245 (2003) 121–137
COORDINATION CHEMISTRY REVIEWS
www.elsevier.com/locate/ccr

Structure and solution behaviour of rhodium(I) Vaska-type complexes for correlation of steric and electronic properties of tertiary phosphine ligands

A. Roodt*, S. Otto[1], G. Steyl

Department of Chemistry and Biochemistry, Rand Afrikaans University, P.O. Box 524, Auckland Park 2006, Johannesburg, South Africa

Contents

Abstract

This paper deals with the synthesis of rhodium(I) Vaska-type complexes of the general form *trans*-$[Rh(CO)X(PX_3)]$ (X = halide, X aryl or alkyl substituent) when incorporating tertiary phosphine ligands and illustrates their simple application as probes to evaluate steric and electronic effects, specifically in tertiary phosphine ligands, analogous to the Tolman model. They are easy to prepare and do not exhibit the toxicity as the corresponding nickel complexes, while structural and infrared data can be conveniently utilised to estimate ligand properties with relative ease. These Vaska-type complexes are often obtained as by-products when reacting $[Rh(\mu\text{-}Cl)(CO)_2]_2$ with bidentate ligands in non-stoichiometric amounts, thus yielding unreacted dimer, which, upon addition of the tertiary phosphine, quantitatively converts to the Vaska-type complex. A representative summary of rhodium(I) Vaska-type systems is reported and structures correlated with steric and electronic properties of related literature complexes. Selected aspects of reactions of the corresponding arsine and stibine analogues are illustrated and solvent effects on equilibrium behaviour as well as the iodomethane oxidative addition described.

Keywords: Vaska-type complexes; *trans*-$[Rh(CO)X(PX_3)]$; Tolman model; Ligand; XXX

* Corresponding author.
E-mail address: aroo@rau.ac.za (A. Roodt).
[1] Current address: Sasol Technology, P.O. Box 1, Sasolburg 1947, South Africa.

0010-8545/$ – see front matter © 2003 Elsevier B.V. All rights reserved.
doi:10.1016/S0010-8545(03)00069-9

1. Introduction

A well-known early organometallic complex, *trans*-[Ir(CO)Cl(PPh_3)$_2$], which was first reported by Angoletta [1], and later correctly formulated by Vaska and DiLuzio [2], is known to exhibit catalytic activity. Interestingly enough, at that time the rhodium analogue was already known [3] and was investigated to some extent [4]. It is thus ironic that today, complexes with the general formula *trans*-[M(CO)Cl(L)$_2$] (M = Rh(I), Ir(I); X = halide or pseudo-halide; L = neutral ligand) are still in many instances known as analogues to Vaska's complex [5,6], in spite of the important earlier contributions in this regard by Chatt and co-workers. Nevertheless, the Vaska-type complexes are typical of those studied by Chatt, which enabled the application of theories that has been developed [7]. These d^8 square-planar systems undergo a range of reactions, such as oxidative addition, with different substrates [5] and were recognised as important model systems for studies on homogeneous catalysis. The rhodium complexes are more resistant towards oxidative addition than their iridium counterparts, and this was believed to be linked to the steric crowding, especially when employing bulky tertiary phosphine ligands, thus hindering the nucleophilic attack of the metal to a substrate molecule. Earlier work by Wilkinson [8–10] explored several aspects regarding the steric and electronic properties of the Rh(I) analogues, but definite crystal structural confirmation of the reaction products could not be achieved.

While organometallic complexes containing tertiary phosphine ligands were extensively studied, the analogous arsine and stibine complexes received very little attention. As a consequence, basic parameters that are well established for phosphine ligands have not been extended to include these ligand systems. Thus, in this paper, some aspects of the electronic and steric properties of arsine [11–13] and stibine [14] ligands are reported.

Selected aspects of novel phosphine ligands, and substituent effects of, e.g., the ferrocenyl fragment, as manifested in the PPh_2Fc ligand [15–18] are also noted. Since not many crystallographic studies on stibine systems have been reported to date [19], in this account, special emphasis is placed on the structural characterisation of the complexes, specifically by detailed crystallographic investigations, as well as the solution equilibria involved in their preparation and isolation. It was also of interest to discuss the solution and solid-state structural effect of arsine and stibine ligands on the oxidative addition reactions of their respective rhodium(I) Vaska-type complexes [13]. Thus, selected aspects address [20] and outline steric implications of analogous Group 15 donor ligands (P, As and Sb)—including the incorporation of methyl substituents on the phenyl rings of these ligands (*p*-Tol = *para*-tolyl; 4-methylphenyl), which results in interesting isomorphic structures.

Two main aspects are involved in the coordination of tertiary phosphine ligands to transition metal atoms. Firstly, the electronic character of the M–P bond is a combined effect of the σ bond formed by donation of the lone pair electron from the P to the M atom and secondly by the ability of the P ligand to accept electron density from the metal by back-donation into a combination of the empty 3d-orbitals and σ*-orbitals of the P atom [21]. A second factor influencing the coordination of a ligand is the spatial demand, or steric size, associated with the specific ligand. In order to rationalise certain parameters, such as steric bulk and electron-donating capability, for ligands with no or very little data available, it is important to cross-reference to other well-known ligand systems, ensuring that all ligands employed are compared on an identical scale. The diversity of tertiary phosphines in terms of their Lewis basicity and bulkiness render them excellent candidates to tune the reactivity of square-planar complexes towards a variety of chemical processes, such as oxidative addition and substitution reactions [22]. A widely quoted parameter to indicate Lewis basicity of tertiary phosphines is the pK_a(H_2O) value thereof, which is a measure of the Brønsted basicity. In general, substituents with better electron-donating capabilities will increase the Lewis basicity of the phosphine, while electron-withdrawing substituents increase the π acceptor ability.

In order to evaluate the electronic characteristics of a specific ligand, one needs a probe, related to electron density in some way, that can be measured conveniently and is sensitive to changes induced in the system by the specific ligand. The effect of tertiary phosphine ligands with different electron-donor and -acceptor capabilities was illustrated by Tolman [23] by measuring, in CH_2Cl_2 medium, the CO-stretching frequency of the *trans* carbonyl group in Ni(0) complexes of the general formula [Ni(CO)$_3$$PR_3$]. These measurements gave a good indication of the relative 'electronic *trans* influences' of the various phosphine ligands. Tolman also found that in this specific system, the electronic measurement was independent of the steric size of the phosphine ligands, a very important factor to keep in mind. Several additional ways of evaluating the electronic properties of phosphine ligands are described in the literature, e.g., the quantitative analysis of ligand effects (QALE) has been extended and developed significantly by Prock and co-workers [24]. Further methods include NMR measurements [25] of first-order Pt–P or P–Se coupling constants, or by measuring the CO-stretching frequency of the rhodium analogues of the Vaska complexes, $\nu(CO_{Rh})$, in solution [26].

The rhodium(I) Vaska-type complexes render themselves as excellent candidates for such a study and several investigations of this nature have been reported before [26]. The advantages of using these complexes include their ease of synthesis, safety, and high degree of stability. Furthermore, the CO-stretching frequency is easily identifiable and gives a sensitive measure of the 'electronic *cis* influence' of the ligands employed. An extensive range

of complexes prepared is thus discussed in order to construct a database from which a correlation is possible to gain some insight into the characteristics of the As and Sb ligands.

This paper, therefore, reports representative rhodium(I) Vaska-type complexes and selected reactions, as primarily studied by our group. It does not intend to cover other metal centres or other reactions studied previously, but simply illustrates the use of these complexes for the estimation of electronic effects, and describes some aspects of the solution behaviour of these systems.

2. Experimental aspects

2.1. General

For experimental procedures utilised in investigations covered by this paper, i.e., synthetic [27,28], UV–vis spectrophotometry [29], kinetic analyses [30], IR/NMR spectroscopy [31] and X-ray crystallography [32], the reader is referred to the earlier work. The data for the crystal structures reported herein were solved using standard techniques and details are reported [33–36]. All IR data reported were collected in chloroform or dichloromethane unless otherwise stated.

In general, the Vaska-type complexes of rhodium(I) containing phosphine and arsine ligands can be conveniently prepared by reacting the rhodium carbonyl chloride dinuclear complex, $[Rh(\mu\text{-}Cl)(CO)_2]_2$, with at least 4 equivalents of the appropriate ligand. In some cases, if very soluble complexes are being formed (typically when using ligands containing alkyl substituents), the reaction medium should be adjusted accordingly to ensure easy isolation of the desired product without contamination by excess ligand.

Practical problems are associated with studying Sb systems such as the resulting uncertainty with regard to elemental analysis reported previously, as well as NMR spectroscopy wherein only poorly resolved proton signals (antimony has two NMR-active isotopes, $I = 5/2$ (57%) and 7/2 (43%), respectively [37], introducing quadrupolar effects) are observed. Moreover, since in this rhodium system the stibine ligands are associated with exchange dynamics, and thus NMR could only be used to a limited extent, X-ray crystallography enabled the unambiguous characterisation of different complexes.

Detailed procedures for the selective preparation of the complexes involving the $SbPh_3$ ligands, to selectively isolate both the red five-coordinate and the yellow four-coordinate complexes, have been described [14]. It is clear that five-coordinate complexes of rhodium are easily formed when utilising stibine ligands and knowledge of the solution behaviour is imperative to manipulate the equilibria in such a way as to favour the formation of the four-coordinate complexes.

2.2. Cone angle calculations

Calculations of the cone angles were done based on the Tolman model [23], but using the actual $Rh–YR_3$ bond distances (Y = P, As, Sb) and angles determined in the crystallographic studies, i.e., the effective cone angles, θ_E, in this case [17,38]. Bond distances of 0.93 Å were assumed for the aromatic C–H hydrogen and a van der Waals radius of 1.2 Å for hydrogen was used in all the calculations.

There are different examples of calculating the steric bulk for specifically tertiary organophosphines [23,39,40], and the review article by Minas de Pidade and co-workers [41] particularly describes aspects in great detail. For simplicity and since it is widely applied, the Tolman model [23] was chosen for the work described in this paper.

3. Steric effects from structural studies on rhodium(I) Vaska-type complexes

Representative Vaska-type complexes of the general form *trans*-$[Rh(CO)Cl(PX_3)_2]$ as obtained from the Cambridge Crystallographic Database [19] are reported in Table 5 in Appendix A. Except for the *trans*-$[Rh(CO)(I)(PX_3)_2]$ [42], there were no reports found on other simple rhodium(I) Vaska-type complexes with other halides, i.e., with analogous bromo of fluoro ligands, that has been structurally characterised.

Selected examples of rhodium(I) Vaska-type complexes, illustrating the square-planar geometry around the rhodium(I) atom, are shown in Fig. 1.

In Fig. 2 is shown an example of an ‘aliphatic’ phosphine, as well as a dinuclear complex containing a Vaska-type fragment. In these structures, the *trans* orientation of Group 15 donor ligands, as well that of the Cl–Rh–CO moiety is obvious. Selected geometrical parameters for a few selected compounds discussed in this paper are reported in Table 1. The dinuclear complex shown in Fig. 2(b) illustrates that Vaska-type fragments can also form under favourable circumstances [44]. A list of dinuclear complexes containing rhodium(I) Vaska-type fragments are thus reported in Table 6 in Appendix A.

The molecular structure of the *trans*-$[Rh(CO)Cl\{As(p\text{-}Tol)_3\}_2]$ complex is shown in Fig. 1(c), and is isomorphous, and thus virtually identical, to the $P(p\text{-}Tol)_3$ analogue [20]. Isomorphism often occurs in these complexes, although definite differences, resulting in a range of polymorphs, have been observed [59]. The $Y(p\text{-}Tol)_3$ complexes (Y = P, As) are of the few structurally characterised Vaska-type complexes not showing a disorder along the carbonyl/chloro axis. The $YR_3(1)–Rh–YR_3(2)$ bond angles for a range of these are 175.69(4)° and 175.67(4)° for $As(p\text{-}Tol)_3$ and $P(p\text{-}Tol)_3$, respectively, which is significantly smaller than 180°, enabling them to crystallise in the non-centrosymmetric space group, $Pna2_1$, and resulting in ‘crystallographic enantiomerically pure’ complexes. The basic geometry of the

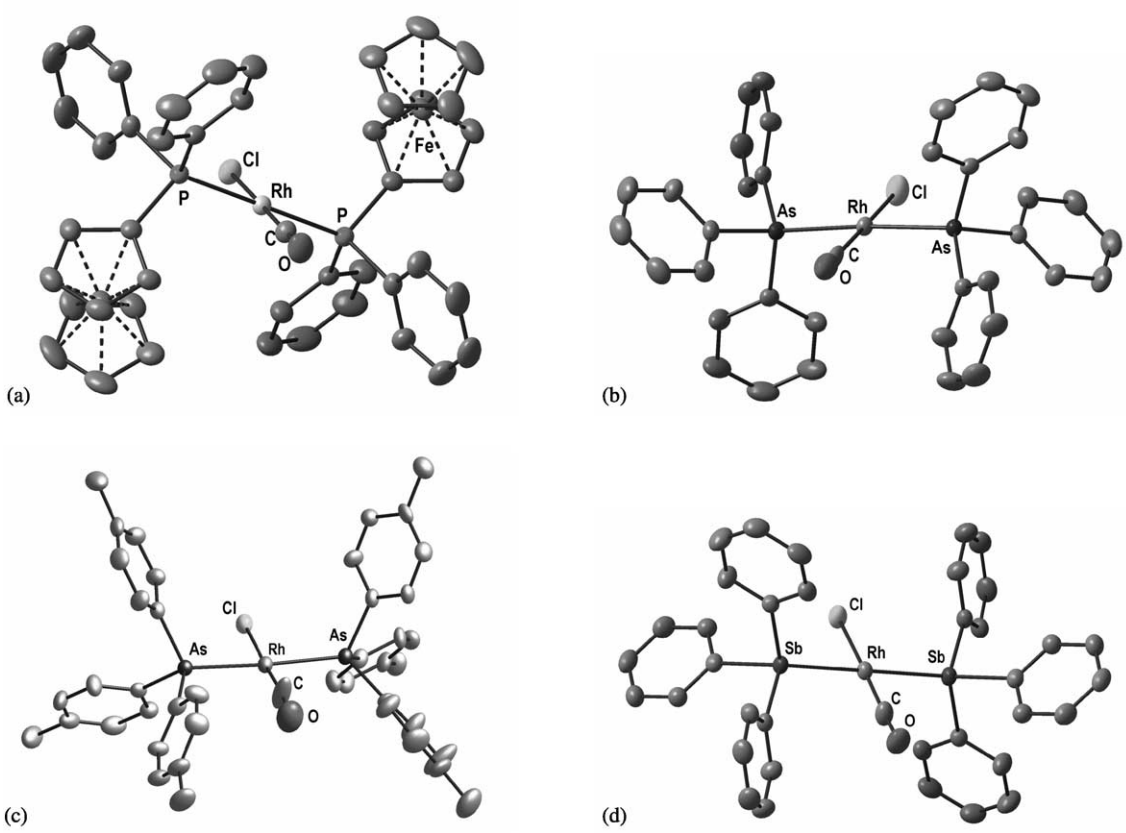

Fig. 1. Diamond drawings of (a) *trans*-[Rh(CO)Cl($PPh_2Fc)_2$] (Adapted from Ref. [43], Copyright: Elsevier, with permission) (b) *trans*-[Rh(CO)Cl($AsPh_3)_2$] (Adapted from Ref. [43], Copyright: Elsevier, with permission) (c) *trans*-[Rh(CO)Cl{As(p-Tol)$_3$}$_2$] (Adapted from Ref. [13], Copyright: Royal Society of Chemistry, with permission) and (d) *trans*-[Rh(CO)Cl($SbPh_3)_2$] (Adapted from Ref. [14], Copyright: Elsevier, with permission) (30% probability ellipsoids; hydrogen atoms omitted for clarity).

molecules, however, stays unchanged. The Flack parameters are zero within experimental error, indicating that the correct stereochemical isomer was refined.

As described earlier [20,32], *trans*-[Rh(CO)Cl{P(*p*-Tol)$_3$}$_2$] is isomorphous to *trans*-[Rh(CO)Cl{As(*p*-Tol)$_3$}$_2$], and they in turn are also isomorphous to *trans*-[Ir(CO)Cl{P(*p*-Tol)$_3$}$_2$] [20], *trans*-[Pt(CH_3)Cl{As(*p*-Tol)$_3$}$_2$] [45] and *trans*-[Ir(CH_3)CO{P(*p*-Tol)$_3$}$_2$] [46] (see Table 1 for selected comparison). This spans a range of different metal centres {along the group, Rh(I) and Ir(I), as well as the period and oxidation states of the metal centre: Ir(I) to Pt(II), the ligands (P and As as donor atoms) and combinations of CO, Cl, and CH_3 *trans* to one another}, and is quite novel. In the case of the corresponding [Rh(CO)(Cl)($YPh_3)_2$] complexes (Y = P, As, Sb), similar isomorphism is not observed [47].

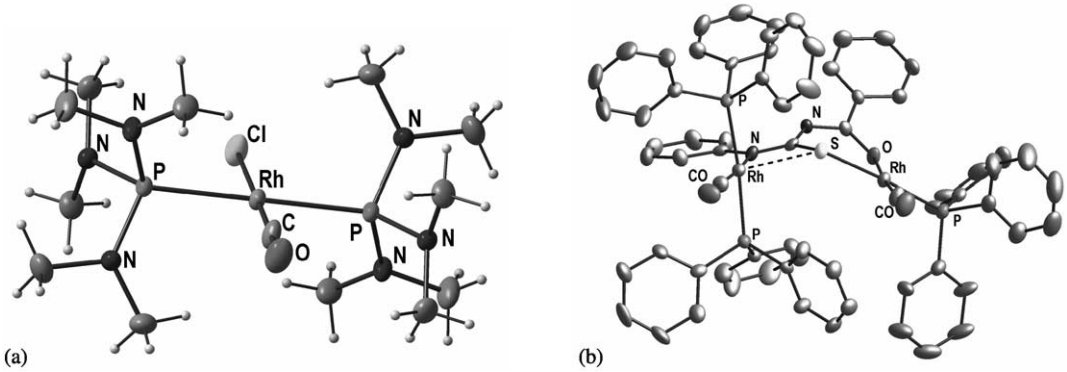

Fig. 2. Diamond drawings of (a) *trans*-[Rh(CO)Cl($P(NMe_2)_2)_3$] (Adapted from Ref. [43], Copyright: Elsevier, with permission) (b) [Rh(CO)(PPh_3)(μ-RRtu)Rh(CO)($PPh_3)_2$] (Adapted from Ref. [44], Copyright: Royal Society of Chemistry, with permission) (30% probability ellipsoids).

Table 1
Comparison of selected bond and spectroscopic data in *trans*-[Rh(CO)(Cl)(L)$_n$] ($n = 2$ or 3) complexes

Complex	Rh–YR$_3$ (Å)	Rh–Cl (Å)	ν(CO) (cm^{-1})	Rh–CO (Å)	C–O (Å)	Y–M–Y (°)	Tolman cone angle of YR$_3$	Reference
[Rh(CO)(Cl)(PPh$_3$)$_2$]	2.322(1)	2.382(1)	1979	1.77(1)	1.140(2)	180.0(1)	145	[48]
[Rh(CO)(Cl)(PCy$_3$)$_2$]	2.3491(7)	2.388(2)	1943	1.748(8)	1.163(7)	180	170	[24]
[Rh(CO)(Cl)(PPh$_2$Fc)$_2$]	2.3344(14)	2.415(7)	1970	1.814(14)	1.056(14)	180	155	[43]
[Rh(CO)(Cl){P(NMe$_2$)$_3$}$_2$]	2.3426(7)	2.443(7)	1964	1.731(9)	1.15(2)	180	168	[43]
[Rh(CO)(Cl){P(*p*-Tol)$_3$}$_2$]	2.333(2)	2.3581(12)	1976	1.798(5)	1.139(6)	175.67(4)	145	[20]
[Rh(CO)(Cl)(PTAMe)$_3$]$^+$	2.344(2)	2.3655(12)	1976	1.798(5)	1.139(6)	175.67(4)	118	[49]
[Rh(CO)(Cl){Babar-Phos}$_2$]	–	–	1991	–	–	–	128	[55],tw [a]
[Rh(CO)(Cl){As(*p*-Tol)$_3$}$_2$]	2.4120(10)	2.347(2)	1973	1.788(10)	1.139(10)	175.69(4)	140	[13]
[Rh(CO)(Cl)(AsPh$_3$)$_2$]	2.4226(4)	2.3538(14)	1975	2.017(7)	0.717(7)	175.97(6)	140	[43]
[Rh(CO)(Cl)(SbPh$_3$)$_2$]	2.5655(2)	2.315(3)	1971	1.797(13)	1.175(13)	180	135	[14]
[Rh(CO)(Cl)(SbPh$_3$)$_3$]	2.5981(5)	2.4094(18)	1971	1.875(7)	1.035(6)	119.97(2)	135	[14]
[Rh(CO)(I)(SbPh$_3$)$_3$]	2.5962(4)	2.7159(8) [b]	1978 [c]	1.825(6)	1.153(6)	180	135	[50]
[Rh(CO)(COCH$_3$)(SbPh$_3$)$_3$]	2.568(2)	–	1710	1.911(20)	1.121(25)	120.0(1)	135	[51]
[IrCl(CO)(PPh$_3$)$_2$]	2.330(1)	2.382(3)	1950	1.791(13)	–	–	145	[51,52]
[IrCl(CO){P(*p*-Tol)$_3$}$_2$]	2.331(2)	2.364(2)	nr [d]	1.817(8)	1.134(10)	175.19(2)	145	[53]
[IrCl(CO)(PCy$_3$)$_2$]	2.345(2)	2.398(7)	1934	1.78(2)	1.10(2)	180	170	[54]

[a] This work, structure as reported assumed.
[b] Rh–I bond distance
[c] Dichloromethane.
[d] Not reported.

In Table 1, a comparison of a range of other relevant *iso*-structural complexes from the literature is also presented. It is clear that significant changes are induced when interchanging ligands. The net effect of introducing larger elements, like the arsine and stibine, is that the steric crowding in the molecule is reduced since it increases some bond lengths, and it thus results in more space for entering moieties in reactions such as substitution and oxidative addition.

As shown in Table 1, the Rh–YR$_3$ bonds (Y = As and P) are longer for the arsine complexes than in the corresponding phosphine analogues. A characteristic feature is that the length of the As–Rh–As moiety is about 4.82 Å, which is significantly longer than the P–Rh–P of 4.66 Å in the P-analogues. This in turn ensures that there is more space available (i.e., a larger 'cavity') for entering nucleophiles in the arsine Vaska-type complex compared to the sterically more hindered phosphine analogue. This has significant consequences for the iodomethane oxidative addition reaction (see Par. 6).

Significant differences in specifically the Rh–Cl bonds are also observed, and since it increases from the P complexes to the As analogues, it suggests less electron density on the Rh-centre in the arsine complexes and a consequent increase in bond Rh–Cl bond strength therein. The Rh–Cl bond length of 2.443(7) Å [Rh(CO)Cl{P(NMe$_2$)$_3$}$_2$] is significantly longer than the others and it is assumed to be indicative of the strong electron donating P(NMe$_2$)$_3$. The Rh–CO and C≡O bond distances in the isomorphous complexes do not differ significantly, although, when statistical disorders are observed, differences might seemingly occur.

Of interest is the fact that the Rh–P and Ir–P bonds in the structures listed in Table 1 are virtually identical (see three final entries of the Ir complexes, compared to the corresponding Rh analogues). However, upon changing the Group 15 donor atom, significant changes in the Rh–L bond length is encountered. In fact, bond lengthening from 2.33 to 2.42 to 2.58 Å from P to As to Sb is introduced—in total ca. a 10% increase. A potential consequence of this is that in the Sb systems, five-coordinate complexes are formed with relative ease. Examples of these are shown in Table 1, which include both the four- and five-coordinate analogues of SbPh$_3$ [47].

To further illustrate the steric effects induced by these tertiary Group 15 ligands, we have calculated the Tolman [23] and the effective cone angles (in the former, θ_T, the fixed 2.28 Å for standardised Ni–P bonds was used, whereas for the effective cone angle, θ_E, the true bond distances were employed [17]). This resulted in θ_T values of 140° and 133° and θ_E values of 140° and 132° for AsPh$_3$ and SbPh$_3$, respectively. The decrease in steric demand as obtained form the 'cavity' described above is thus also further underlined by the decrease in θ_T and θ_E of more than 10° compared to that of PPh$_3$ (assuming the cone angles for *para*-substituted phenyl phosphines to be virtually identical to PPh$_3$ as such). Coupled with this decrease in steric demand are additional factors of importance, such as the increase introduced in the P–C, As–C and Sb–C bond lengths, ranging from 1.82 to 1.94 to 2.10 Å [14,43]. The changes in bond lengths and tetrahedral angles are thus in accordance with the covalent radii of these elements, i.e., N (0.70), P (1.10), As (1.21), Sb (1.41) and Bi (1.47 Å). Furthermore, the C–L–C tetrahedral angles for the Group 15 elements were reported as 116°, 109°, 102°, 97° and 94° for N to Bi, respectively [56], which results in an increased 'folding back' ability of larger substituents from the M–L bond direction.

The Tolman cone angle for the polycyclic phosphirane ligand termed $^{i\mathrm{Pr}}$Babar-Phos by Grützmacher and co-workers

[57,58] was estimated to be 128° (see Table 1). Of interest is that the 'Babar'-fragment, i.e., the heterocycle, contributes only ca. 2 × 38° (half-angles) to the steric demand as defined by Tolman, whereas the *iso*-propyl fragment contribution is ca. 53°.

4. Electronic effects from spectroscopy

4.1. Phosphorous 31-NMR

Since the phosphorous-31 and the rhodium-103 isotopes both have the same nuclear spin ($I = 1/2$) and are 100% abundant, first-order coupling constants observed by ^{31}P-NMR yields valuable information. The reader is referred to previous reports [29,31] covering this on the square-planar [Rh(L,L′-BID)(CO)(PX$_3$)] complexes, which can be considered close 'relatives' of the Vaska-type ones. In fact, aspects in this regard, establishing even closer links with the Vaska-type complexes, are discussed in Par. 5.

However, for the simple rhodium(I) Vaska-type complexes as such, the correlation is not good since bonding modes of the *trans* phosphine ligands appear to be similar (see Table 1). Selected bond distances of a range of these complexes are also reported therein.

Table 2
Infrared data (CH_2Cl_2) for [Ni(L)(CO)$_3$] and *trans*-[RhCl(CO)(L)$_2$] complexes

	L	ν(CO$_{Ni}$) (cm^{-1})	ν(CO$_{Rh}$) (cm^{-1})
1	PCy_3	2056.4	1943
2	P^iPr_3	2059.2	1950
3	$AsEt_3$	2059.6 [47]	1954
4	P^nBu_3	2060.3	1955
5	$PPhFc_2$	2060.5 [47]	1957
6	PEt_3	2061.7	1958
7	$P(NMe_2)_3$	2061.9	1964
8	$PPhEt_2$	2063.7	1964
9	$PPhCy_2$	2060.6	1964
10	PPh_2Cy	2064.8	1966
11	PPh_2Me	2067.0	1968
12	PBz_3	2066.4	1970
13	PPh_2Fc	2065.5 [47]	1970
14	$SbPh_3$	2065.8 [47]	1971
15	PPh_2Et	2066.7	1973
16	As(*p*-Tol)$_3$	2066.8 [47]	1973
17	P(*o*-Tol)$_3$	2066.6	1974
18	$AsPh_3$	2067.9 [47]	1975
19	P(*p*-OMe-Ph)$_3$	2066.1	1975
20	P(*p*-Tol)$_3$	2066.7	1976
21	PPh_2(*p*-Tol)	2068.2	1977
22	PPh_3	2068.9	1979
23	$PPh_2(C_6F_5)$	2075.9	1983
24	P(*p*-F-Ph)$_3$	2071.3	1983
25	P(*p*-Cl-Ph)$_3$	2072.8	1983
26	Babar-Phos	2078.4 [a]	1991
27	PPh_2Cl	2080.7	1993
28	$PPh(C_6F_5)_2$	2082.8	1996
29	$P(C_6F_5)_3$	2090.9	2005

[a] Obtained from Fig. 3.

4.2. Infrared spectroscopy

The IR data for a range of rhodium(I) Vaska-type complexes are listed in Table 2, and it is clear that a good correlation exists between that of the nickel(0) and the rhodium(I) Vaska-type complexes. It is clear that the ν(CO$_{Rh}$) values cover almost twice the range than the ν(CO$_{Ni}$) values with $\Delta\nu$(CO$_{Rh}$) = 62 cm^{-1} and $\Delta\nu$(CO$_{Ni}$) = 35 cm^{-1}. The ν(CO$_{Ni}$) vs. ν(CO$_{Rh}$) data for the range of the rhodium(I) Vaska-type complexes reported in Table 2 were fitted to a simple quadratic equation as shown in Fig. 3.

Tolman rationalised the measurements on the [Ni(CO)$_3$L] complexes in terms of Eq. (1) which is conveniently used to calculate the electronic parameter ν(CO$_{Ni}$) for phosphine ligands containing common substituents.

$$\nu(\mathrm{CO_{Ni}})\ \text{for}\ \mathrm{PX_1X_2X_3}:\ \nu(\mathrm{CO_{Ni}}) = 2056.1 + \sum_{i=1}^{3}\chi_i \quad (1)$$

In Eq. (1), each substituent has a value for χ (^{t}Bu = 0; Cy = 0.1; Et = 1.8; Ph = 4.3, etc.) that has to be known to calculate the value of ν(CO$_{Ni}$). This equation implies that P(^{t}Bu)$_3$ has the highest electronic *trans* influence (strongest electron donor) and on replacing the ^{t}Bu groups with other groups, a correction must be applied since a decrease in the *trans* influence causes an increase in the CO-stretching frequency. This observation is best explained as a result of a decrease in electron density on the metal centre giving rise to poorer back-donation from the metal into the anti-bonding orbital on the C atom. The decrease in the back-donation results in a weaker Rh–C bond and thus a stronger CO bond which in turn results in an increase in the CO-stretching frequency. For comparison, it is obvious to determine the values of ν(CO$_{Rh}$) in solution since packing effects have

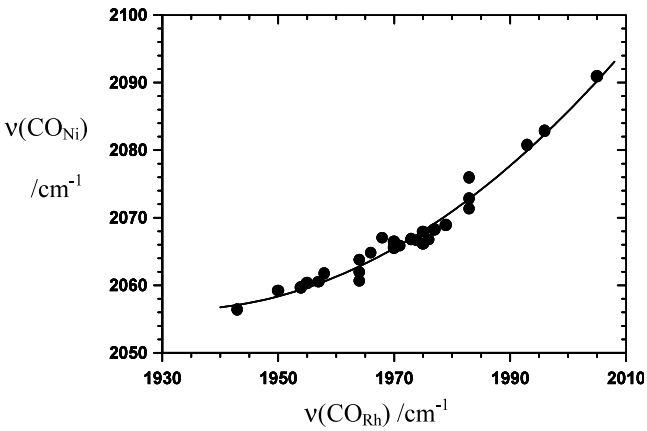

Fig. 3. Correlation between ν(CONi) and ν(CORh) for all complexes in Table 2 [nonlinear least-squares fit of data to simple quadratic function; $y = ax^2 + bx + c$; $a = (2.77 \pm 0.44) \times 10^4$, $b = (-2.65 \pm 0.45) \times 10$, $c = (6.8 \pm 1.1) \times 10^{-3}$].

been illustrated to have a significant influence on the value rendering solid-state measurements useless [59].

Fig. 3 provides an easy way to cross-correlate new ligands. For example, substituting, the $\nu(CO_{Ni})$ value for PPh_2Fc (2065.4 cm^{-1}) obtained from Fig. 3 into Eq. (1) and solving ($\chi_{Ph} = 4.3$) gives: $2065.4 = 2056.1 + 2(4.3) + \chi_{Fc}$; thus $\chi_{Fc} = 0.7$. This χ value of 0.7 for the ferrocenyl substituent indicates it to be a good electron-donating group, comparable to *o*-C_6H_5OMe ($\chi = 0.9$).

The corresponding $\nu(CO_{Ni})$ values for, e.g., the PPh_2Fc, BaBar-Phos and different As- and Sb-ligands could thus be obtained with relative ease using Fig. 3, Eqs. (1) and (2).

To determine the contributions of As and Sb relative to P-ligands, an additional term correcting for the donor atom (C_L) was added to Eq. (1) thus giving Eq. (2):

$$\nu(CO_{Ni}) = 2056.1 + \sum_{i=1}^{3} \chi_i + C_Y \quad (2)$$

According to definition, the phosphine ligands have $C_P = 0$. Substituting the $\nu(CO_{Ni})$ values for $AsEt_3$ (2059.6), As(*p*-$C_6H_5Me)_3$ (2066.9), $AsPh_3$ (2068.0) and $SbPh_3$ (2065.9) obtained from Fig. 3 into Eq. (2) and solving gave the following values for $C_{As} = -1.9$ ($AsEt_3$), $+0.3$ (As(*p*-$C_6H_5Me)_3$) and -1.0 ($AsPh_3$), and $C_{Sb} = -3.0$ ($SbPh_3$). From these results, the C_{As} value of $+0.3$ obtained for As(*p*-$C_6H_5Me)_3$ seems a bit strange compared to the negative values obtained for the other As ligands. Direct subtraction of the $\nu(CO_{Rh})$ values of As(*p*-$C_6H_5Me)_3$ and P(*p*-$C_6H_5Me)_3$ gives $1973 - 1976 = -3$ cm^{-1} and dividing with 2 to convert to the smaller range for $\nu(CO_{Ni})$ suggest a value of -1.0 to -1.5 cm^{-1}. Based on these arguments, an average value of -1.5 is proposed for C_{As} and the values of -3.0 is retained for C_{Sb}.

As the electron-donating capability of the Group 15 donor L-ligand decreases, the electron density on the metal decreases accordingly and thus less electron density is available to the C≡O moiety via π-back-bonding into the carbon π*-orbitals. The result is a weaker M−CO bond (stronger C≡O bond) and an increase in ν(CO). This is evident for complexes listed in Table 1. The change in ν(CO) introduced from P to As to Sb for PPh_3, $AsPh_3$ and $SbPh_3$ is 1979, 1975 and 1971 cm^{-1}, respectively, which is not very large, but still significant. The net change in electron density is additionally illustrated by the reactivity change of the oxidative addition for the complexes presented here (Table 4).

Of interest is the fact that the ligand termed ^{i}PrBabar-Phos by Grützmacher and coworkers [57,58], and designed to be a very weak electron donor, indeed shows characteristics comparable to the halogenated phosphines, i.e., a $\nu(CO_{Rh})$ of 1991 cm^{-1}, which translates to a Tolman electronic parameter, $\nu(CO_{Ni})$ of 2078 cm^{-1}.

It has to be remembered that, as illustrated, many factors influence the $\nu(CO_{Rh})$ values, and it is thus still at best a rough estimate of illustrating tendencies for these systems.

5. Five-coordinate rhodium(I) Vaska-type complexes

Vaska-type complexes are, illustrated above, usually considered as four-coordinate. However, under favourable conditions, an additional ligand can be added to the metal centre to retain or from the typical *trans*-YR_3 Vaska-type fragment. Thus, decrease in steric crowding, and an accompanying decrease in electron density introduced to the rhodium(I) centre, favours the formation of five-coordinate Vaska-type complexes. Two selected examples are discussed below.

5.1. Complexes of the type [Rh(CO)Cl(YR_3)$_3$]

5.1.1. Structural studies

Five-coordinate complexes of the Vaska-type, containing ligands with non-phosphorus group 15 donor atoms, are not common. Particularly, complexes containing stibine ligands have only been investigated to a very limited extent since phosphine complexes are in general favoured on the basis of the NMR activity of phosphorous. Furthermore, large variations of phosphine ligands are commercially available, enabling broad studies without time-consuming ligand synthesis involving extremely hazardous chemicals. Thus, different attempts to prepare and characterise the rhodium stibine analogue to Vaska's complex are reported in the literature [3,60,61], of which several are incorrect.

For example, early work on the synthesis of $SbPh_3$ complexes of rhodium(I) [3] described rhodium complexes containing three stibine ligands. The colour of the complexes was reported to range from orange red to purple red, whereas the analogous phosphine- and arsine-containing complexes are yellow. Molecular mass determinations and elemental analysis suggested the stibine complexes to be the four-coordinate analogues of the rhodium phosphine complexes that were already known at that time. Two more accounts by other authors describing the rhodium stibine complexes as having red colours also appeared during that time [60,61]. A brief correction that was given in a footnote was the first report of these complexes to be five-coordinate and containing three stibine ligands [62]. Confirmation of the presence of three stibine ligands by elemental analysis and the existence of solution equilibria between the four- and five-coordinate rhodium complexes appeared shortly afterwards [63]. Practical problems concerning the elemental analyses were mentioned and the presence of an additional benzene molecule in all the synthesised complexes raised some questions concerning these results. The first reference to the preparation of the yellow four-coordinate complex is only sited as a personal communication [63,64].

Clearly, some confusion existed with regard to the solution behaviour of the stibine systems, since an equilibrium as outlined above and given in Eq. (3), exists. To confirm this, both the reactant and the product were isolated and structurally characterised (see Figs. 1(d) and 4(a)). Thus, the difficulty associated with interpreting NMR spectra of As and Sb complexes (unfavourable properties of the nuclei)

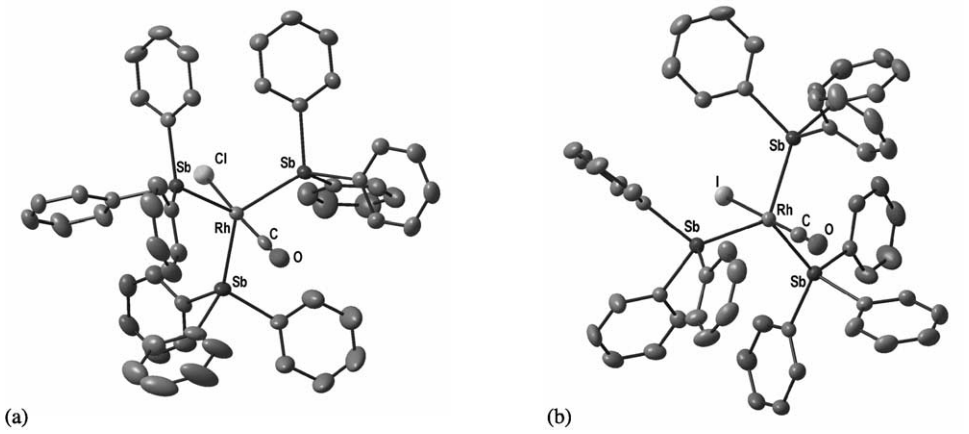

Fig. 4. Diamond drawings of (a) *trans*-[Rh(CO)Cl($SbPh_3$)$_2$] (Adapted from Ref. [14], Copyright: Elsevier with permission) and (b) *trans*-[Rh(CO)I($SbPh_3$)$_2$] (Adapted from Ref. [50], Copyright: Elsevier, with permission) (30% probability ellipsoids; hydrogen atoms omitted for clarity).

has been partially circumvented by X-ray structural analysis and UV–vis spectrometric measurements (see below).

$$[Rh(CO)Cl(SbPh_3)] + SbPh_3 \overset{K_f}{\rightleftarrows} [Rh(CO)Cl(SbPh_3)_3] \quad (3)$$

The corresponding iodo analogue of the tris–$SbPh_3$ complex has also been reported recently (see Fig. 4(b) and Table 1).

Another recent interesting example, utilising again a P-donor in the ligand the methylated 1,3,5-triaza-7-phosphaadamantane ($PTAMe^+$) which is very weakly electron donating (positive charge), is shown in Fig. 5 and selected geometrical data are given in Table 1. It is concluded that five-coordination in these systems is favoured by electrophilic metal centres with small steric crowding at the metal [49].

5.1.2. Formation constant studies

Equilibrium constants for the formation of *trans*-[Rh(CO)Cl($SbPh_3$)$_3$] (Eq. (3)) in different solvents have been studied, of which least-squares fits of the absorbance data changes are shown in Fig. 6. The solutions turned from the initial yellow colour of the *trans*-[Rh(CO)Cl($SbPh_3$)$_2$] into the dark red colour characteristic of the *trans*-[Rh(CO)Cl($SbPh_3$)$_3$] with an increase in the $SbPh_3$ concentration. The progressive increase of the stability constant in the five solvents is clearly illustrated in Table 3.

The formation constants determined in different solvents according to Eq. (3) (also see Scheme 2) in Scheme 1 indicate that the formation of the *bis*-$SbPh_3$ complex is more favoured in less polar/non-coordinating solvents. In fact, there is almost an order of magnitude difference in the *K*(dcm) value vs. those obtained in acetone and ethyl acetate (Table 3). It is, however, not certain whether the inherent solvent characteristics (donicity, polarity) are necessarily the only reason for isolation of *trans*-[Rh(CO)Cl($SbPh_3$)$_2$]. A lower crystallisation energy of the latter compared to the tris–$SbPh_3$ complex in solvents such as diethyl ether and hexane obviously adds some driving force for obtaining the four-coordinate complex. The solubility of *trans*-[Rh(CO)Cl($SbPh_3$)$_2$] in diethyl ether is <0.2 mM, thus the success of the synthetic method is supposedly driven

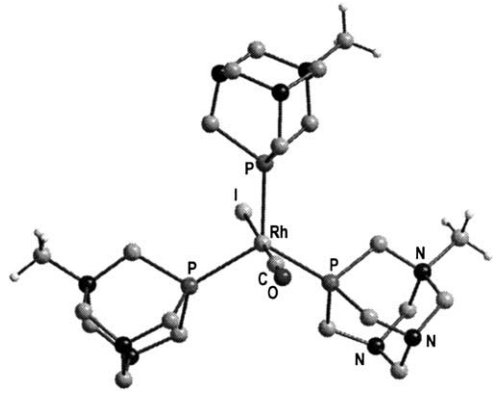

Fig. 5. Diamond drawings of *trans*-[Rh(CO)I($PTAMe)_3]^{3+}$ (Adapted from Ref. [49], Copyright: Elsevier, with permission) (30% probability ellipsoids; hydrogen atoms omitted for clarity).

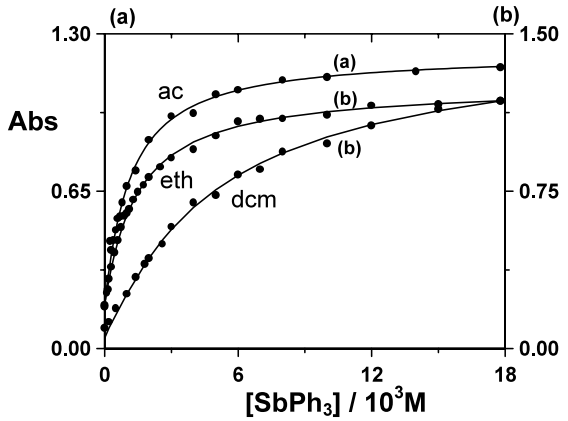

Fig. 6. Least-squares fits (lines) of absorbance change vs. [$SbPh_3$] for the formation of *trans*-[Rh(Cl)(CO)($SbPh_3$)$_3$] (Scheme 1) in acetone (ac, 450 nm), diethyl ether (eth, 420 nm), dichloromethane (dcm, 450 nm), at 25 °C (Adapted from Ref. [14], Copyright: Elsevier, with permission).

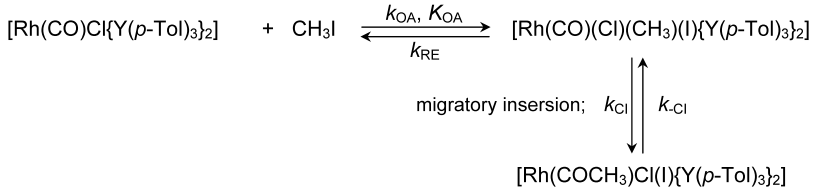

Scheme 1.

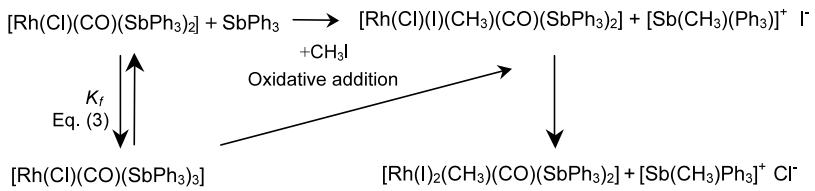

Scheme 2.

Table 3
Formation constants for *trans*-[Rh(CO)Cl(SbPh$_3$)$_3$] (Eq. (3)) in different solvents at 25 °C

Solvent	D_N [a]	D_S [b]	ε [c]	K_f [d] (M^{-1})
Dichloromethane	4 [e]	6	8.9	163 ± 8
Benzene	0.1	9	2.3	363 ± 7
Nitromethane	2.7	9	35.8	>200 [f]
Diethylether	19	12	4.3	744 ± 34
Acetone	17	15	20.7	1043 ± 95
Ethyl acetate	17	14	6.0	1261 ± 96

[a] D_N = donor number [65].
[b] D_S = donor strength [66].
[c] ε = dielectric constant [67].
[d] Fig. 4.
[e] Estimated from chloroform.
[f] Estimated value; significant decomposition.

by the favourably low energy of crystallisation, even though the stability constant in this solvent is quite large (Table 3).

Thus, given the appropriate conditions and if a suitable ligand is available, these Rh(I) systems will add a fifth ligand in order to compensate for this lack of electron density.

5.2. Complexes of the type [Rh(L,L′-BID)(CO)(YR$_3$)$_2$]

Systems of the form [Rh(L,L′-BID)(CO)(YR$_3$)$_2$] that contained a five-membered monocharged bidentate ligand (L,L′-BID), such as cupferrate [68] or tropolonate [69] and derivatives [70], showed a tendency to accommodate an additional phosphine/arsine ligand (YR$_3$) (Eq. (4)). It thus forms distorted trigonal-bipyramidal complexes containing the basic Vaska-type fragment. An example of a structurally characterised complex of this type is shown in Fig. 7 [69].

$$[\mathrm{Rh(L,L'\text{-}BID)(CO)(YR_3)}] + \mathrm{YR_3} \overset{K_f}{\rightleftarrows} [\mathrm{Rh(L,L'\text{-}BID)(CO)(YR_3)_2}] \quad (4)$$

The formation constants for the reaction shown in Eq. (4) (L,L′-BID=tropolonate) were determined as 30(4), 57(9) and 53(8) M^{-1} for PPh$_2$Fc, PPh$_3$ and P(*p*-FPh)$_3$, respectively [69]. This indicated that the electron density introduced synergistically by the two *trans*-YX$_3$ ligands was not significantly different. Corresponding structures of systems containing six-membered oxygen donor atoms have not been reported, possibly indicating steric hindrance by the L,L′-BID ligand playing an important role in the formation of these five-coordinate complexes.

The formation constant described for the HtropBr$_3$ according to Eq. (4) increased by approximately an order-of-magnitude for both the PPh$_3$ and AsPh$_3$, thus indicating that the tendency to form the five-coordinate complex is directly related to the electron density (or lack thereof) on the rhodium(I) as introduced by the bidentate ligand. Thus, when additional electron-withdrawing capacity was introduced on the L,L′-BID ligand, as in the case of the 3,5,7-tribromotropolone (HtropBr$_3$), the formation of both the PPh$_3$ and AsPh$_3$ complexes are favoured and could be isolated and crystallographically studied [70] as shown in Fig. 8. Of further interest is the fact that [Rh(tropBr$_3$)(CO)(YPh$_3$)$_2$] (Y = P, As) complexes are isomorphous, and there is a significant distortion in the solid state towards square-pyramidal geometry. Thus, although tropBr$_3^-$ is a symmetrical ligand, the Rh–O1 and Rh–O2

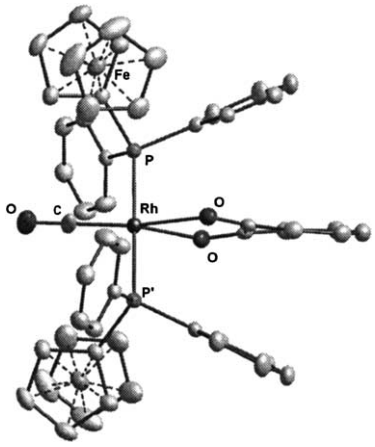

Fig. 7. Diamond drawing of *trans*-[Rh(CO)(trop)(PPh$_2$Fc)$_2$] (Ref. [69]) (30% probability ellipsoids; hydrogen atoms omitted for clarity).

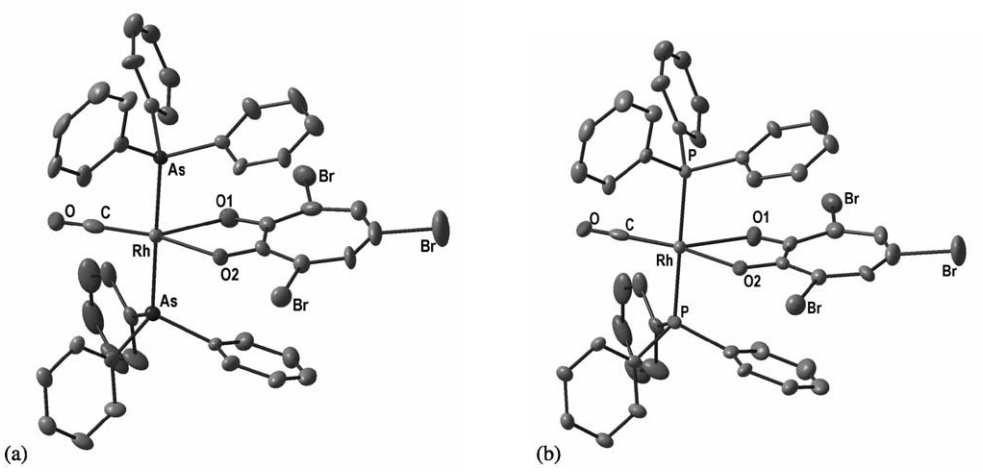

Fig. 8. Diamond drawings of (a) *trans*-[Rh(CO)(tropBr$_3$)(PPh$_3$)$_2$] [70] and (b) *trans*-[Rh(CO)(tropBr$_3$)(AsPh$_3$)$_2$] [70] (30% probability ellipsoids; hydrogen atoms omitted for clarity).

(virtually trans to the Co ligand) in both the structures shown in Fig. 8 were ca. 2.46–2.48 and 2.16 Å, respectively. However, in the case of the [Rh(trop)(CO)(PPh$_2$Fc)$_2$], these bonds were identical (two-fold axis along the Rh–CO bond in Fig. 7). The corresponding decrease in bite angle from 68.88(9)° in the bis-PPh$_2$Fc complex shown in Fig. 7, compared to the 66.7(2) and the 66.8(2)° in the five-coordinate PPh$_3$ and AsPh$_3$ complexes shown in Fig. 8 attributed to this assymetric distortion, is quite significant. The Rh–P and Rh–As bond lengths in these five-coordinate tropBr$_3$ complexes are 2.337(2) and 2.412(1) Å, respectively, and compare well with the corresponding bond distances in the four-coordinate Vaska analogues listed in Table 2, [Rh(CO)Cl(YPh$_3$)$_2$] and [Rh(CO)Cl{Y(*p*-tol)$_3$}$_2$], displaying values for Rh–P, 2.322(1) and 2.333(2) Å, and Ph–As, 2.4226(4) and 2.412(1) Å, respectively. This observation indicates that the group 15 donor atom (Y) is the prime determinate factor regarding the Rh–Y bond, and that the Rh–Y bond variation is fairly insensitive toward substituents on the Y-atom, as well as the ligand (i.e., Cl$^-$ or trop$^-$) on the metal centre 'trans' to the carbonyl moiety. Preliminary energy calculations showed that the more stable state is in fact the distorted square-pyramidal, and not the trigonal-bipyramidal shown in Fig. 7. Further investigation into this, as well as other aspects relevant to the factors determining the formation of these five-coordinate complexes, is obviously still needed.

6. Iodomethane oxidative addition on rhodium(I) Vaska-type complexes

6.1. Reactions of the trans-[Rh(CO)Cl{Y(p-Tol)$_3$}$_2$] (Y = P, As) complexes

Upon reaction of rhodium(I) Vaska-type complexes with iodomethane, the metal centres are typically alkylated followed by subsequent migratory insertion, similar to that reported for the [Rh(L,L′-BID)(CO)(PX$_3$)] complexes [29]. Thus, in this paper, selected aspects of these reactions, aimed at the rhodium(I) Vaska-type complexes containing monodentate ligand systems, are briefly discussed. Representative data for iodo carbonyl complexes of rhodium(I) and rhodium(III) are given in Table 7 in Appendix A.

For the reaction of the iodomethane oxidative addition to the *trans*-[Rh(CO)Cl{Y(*p*-Tol)$_3$}$_2$] (Y=P, As), the general stoichiometry of the reaction is shown in Scheme 1. The equilibrium reaction defining the first step (forward = oxidative addition; reverse = reductive elimination) was verified previously [10,29], but is also illustrated in Fig. 9.

The slow decomposition of the *trans*-[Rh(CO)Cl{As(*p*-Tol)$_3$}$_2$] complex in Fig. 9 (ν(CO) = 1973 cm^{-1}), and the clean conversion to the intermediate alkyl species (ν(CO) = 2050 cm^{-1}), is obvious. However, under identical

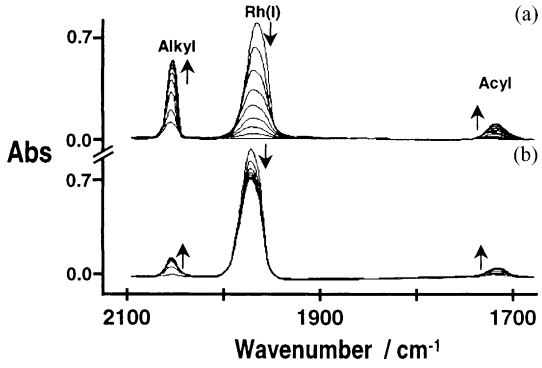

Fig. 9. Infrared spectra (25 °C, 10-min intervals) of iodomethane oxidative addition to (a) *trans*-[Rh(CO)Cl{As(*p*-Tol)$_3$}$_2$] and (b) *trans*-[Rh(CO)Cl{P(*p*-Tol)$_3$}$_2$], illustrating the formation of the Rh(III)-alkyl and Rh(III)-acyl species; CHCl$_3$, [Rh] = 0.02 M; [CH$_3$I] = 3 M (Adapted from Ref. [13], Copyright: The Royal Society of Chemistry, with permission).

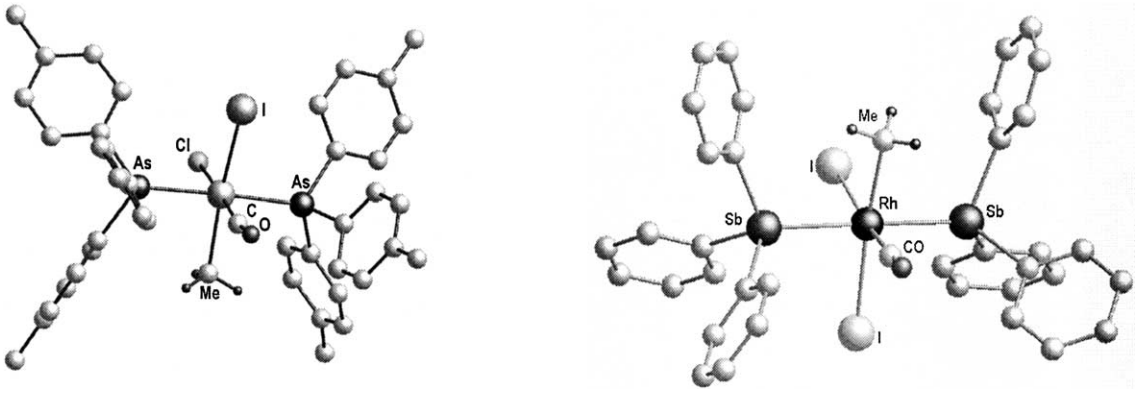

Fig. 10. Diamond drawings of (a) *trans*-[Rh(CO)(Cl)I(Me){As(*p*-Tol)$_3$}$_2$] (Ref. [13], with permission) and (b) *trans*-[Rh(CO)(I)$_2$(Me)(SbPh$_3$)$_2$] (Adapted from Ref. [14], Copyright: Elsevier:, with permission).

conditions in the case of the *trans*-[Rh(CO)Cl{P(*p*-Tol)$_3$}$_2$] complex, only a small amount of the reactant is converted to the intermediate alkyl species, thus confirming the thermodynamic unfavourability of the latter. This might explain why the intermediate P-alkyl complex could not be isolated, compared to the corresponding As species, which has indeed been obtained in the solid state and structurally characterised (see Fig. 10(a)).

The molecular structure of [Rh(CO)Cl(CH$_3$)(I){As(*p*-Tol)$_3$}$_2$] shown in Fig. 10(a) clearly shows that *trans* addition of the iodomethane occurred. In the past decade, a range of alkyl intermediates in iodomethane oxidative addition to rhodium(I) complexes has been isolated and it has been found in general that in sterically congested and electron-rich metal centres systems, the *trans* products were isolated [29].

[Rh(CO)Cl(CH$_3$)(I){As(*p*-Tol)$_3$}$_2$] represents one of the very few characterised arsine complexes of this type, and of interest is the fact that the Rh–As bonds were lengthened by almost 0.05 Å compared to the starting material [Rh(CO)Cl{As(*p*-Tol)$_3$}$_2$] (Fig. 1(c)). This subsequently increases the As–Rh–As cavity from 4.835(1) to 4.959(2) Å in [Rh(CO)Cl(CH$_3$)(I){As(*p*-Tol)$_3$}$_2$], but the Rh–Cl bond stayed virtually unaffected. Moreover, the Rh–CO bond length increased, in spite of the fact that the e.s.d. is quite large and suggests that the apparent lengthening should thus be interpreted with care. However, the tendency of significant bond length increase cannot be overlooked, which is in agreement with the higher ν(CO) value of 2050 cm^{-1}, indicative of much less d–π^* electron back-donation from the Rh(III) metal centre.

By comparison, the Rh–I bond distance of 2.786(1) Å is quite long (*trans* to a methyl) relative to the 2.708(2) and 2.701(1) Å found for Rh(III)–I bonds (i.e., a *trans*-P–Rh–I moiety) in [Rh(cupf)I(CH$_3$)(CO)(PPh$_3$)] [71] and [Rh(quin)I(CO)(CH$_3$)(PPh$_3$)] [72] (*cis* addition of iodomethane, cupf = cupferrate; quin = quinolinate). It is, however, significantly shorter than other Rh–I bond lengths in complexes containing *trans*-CH$_3$–Rh–I moieties, e.g., the 2.803(1) Å in [Rh(ox)I(CO)(CH$_3$)(PPh$_3$)] (average of two crystallographically independent molecules; ox = 8-hydroxyquinolinate) [73] and especially the 2.849(1) Å in [Rh(dmavk)I(CO)(CH$_3$)(PPh$_3$)] (dmavk = dimethylaminovinylketonate) [74]. In the latter two examples, the metal centres were quite nucleophilic (reactivity toward iodomethane high; half-lives at [CH$_3$I] = 1 M in second range). The fact that a shorter Rh–I bond in [Rh(CO)Cl(CH$_3$)(I){As(*p*-Tol)$_3$}$_2$] was observed compared to these more reactive rhodium(I) complexes thus suggests a stronger coordination of the iodo ligand due to less electron density on the metal centre. This is in general agreement with the slow kinetics observed for iodomethane oxidative addition to [Rh(CO)Cl{Y(*p*-Tol)$_3$}$_2$] as discussed below.

6.2. Reactions of the trans-[Rh(CO)Cl(SbPh$_3$)$_2$] and trans-[Rh(CO)Cl(SbPh$_3$)$_3$] complexes

The equilibrium that exists between the four- and five-coordinate SbPh$_3$ complexes as described above complicate the oxidative addition reaction as indicated by Scheme 2.

After dissolving *trans*-[Rh(CO)Cl(SbPh$_3$)$_3$] in acetone, a mixture of the bis and tris complexes, *trans*-[Rh(CO)Cl(SbPh$_3$)$_2$] and *trans*-[Rh(CO)Cl(SbPh$_3$)$_3$], is formed, accompanied by the liberation of SbPh$_3$. Addition of CH$_3$I to such a solution results in CH$_3$I oxidative addition not only to the bis and tris SbPh$_3$ complexes, but also to the liberated SbPh$_3$, thus forming [SbMePh$_3$]I. The [SbMePh$_3$]I thus produced acts as a source of I$^-$ ions to substitute the Cl$^-$ from the rhodium metal centre, resulting in *trans*-[Rh(CO)(I)$_2$(Me)(SbPh$_3$)$_2$] as the final product (see Fig. 10(b)).

The fact that *trans*-[Rh(CO)Cl(SbPh$_3$)$_3$] undergoes oxidative addition with CH$_3$I to form a Rh(III) complex containing only two SbPh$_3$ ligands coordinated to the metal centre in the final product is in contrast to a recent study [75] where the reaction of the former with HC≡CCH$_2$Cl gave [Rh(Cl)(η^2-C(=O)CH=CClCH$_2$)(SbPh$_3$)$_3$] as final product. In this case, the dissociated SbPh$_3$ ligand re-coordinated to the Rh(III) oxidative addition product, following cycload-

Table 4
Kinetic results for iodomethane oxidative addition to *trans*-[Rh(CO)Cl{Y(*p*-$C_6H_4CH_3$)$_3$}$_2$] (Y = As and P) at 25 °C[a]

Complex	Constant	Acetone	Ethyl acetate	DCM	Toluene
	ε [b]	20.7	6.0	8.9	2.38
	D_N [c]	17.0	17.1	4 [d]	0.1 [e]
P	$10^3 k_{OA}$ ($M^{-1} s^{-1}$)	1.30(6)	0.26(1)	2.90(9)	0.20(1)
	$10^3 k_{RE}$ (s^{-1})	0.75(2)	0.880(3)	1.27(4)	1.63(2)
	K_{OA} (M^{-1})	1.7(1)	0.30(1)	2.3(1)	0.120(6)
	$\Delta H^{\#} k_{OA}$ (kJ mol^{-1})	58(3)	–	71(12)	–
	$\Delta S^{\#} k_{OA}$ (J K^{-1} mol^{-1})	−100(9)	–	−47(30)	–
	$\Delta H^{\#} k_{RE}$ (kJ mol^{-1})	39(4)	–	30(12)	–
	$\Delta S^{\#} k_{RE}$ (J K^{-1} mol^{-1})	−167(14)	–	−193(40)	–
As	$10^3 k_{OA}$ ($M^{-1} s^{-1}$)	4.2(4)	0.84(1)	0.60(1)	0.05(2)
	$10^3 k_{RE}$ (s^{-1})	0.52(6)	5.11(5)	0.041(4)	0.445(2)
	K_{OA} (M^{-1})	8(1)	0.160(7)	15(1)	0.11(4)
	$\Delta H^{\#} k_{OA}$ (kJ mol^{-1})	84(1)	114(4)	87(6)	–
	$\Delta S^{\#} k_{OA}$ (J K^{-1} mol^{-1})	−1(4)	86(15)	−8(18)	–
	$\Delta H^{\#} k_{RE}$ (kJ mol^{-1})	53(1)	83(6)	–	–
	$\Delta S^{\#} k_{RE}$ (J K^{-1} mol^{-1})	−122(5)	−3(18)	–	–
Sb	$10^3 k_{OA}$ ($M^{-1} s^{-1}$)	–	–	0.12(1)	–
	$10^3 k_{RE}$ (s^{-1})	–	–	0.0015(4)	–
	K_{OA} (M^{-1})	–	–	100(20)	–

[a] [13].
[b] [65].
[c] [66].
[d] Estimated from chloroform.
[e] Estimated from benzene.

dition and Cl^- migration, to retain a saturated coordination sphere. In CH_3I oxidative addition to the dissociated $SbPh_3$, the resulting formation of $[SbMePh_3]^+ I^-$, effectively scavenges $SbPh_3$ as potential ligand from the reaction medium. The exact sequence of reactions as well as the reactivity of different species toward iodomethane oxidative addition in this complicated mechanism are not resolved at this stage.

6.3. Rate laws for iodomethane oxidative addition to rhodium(I) Vaska-type complexes

It has been shown previously [10,29] that the iodomethane oxidative addition to rhodium(I) complexes proceed according to the general mechanism as given in Scheme 1. The forward step in the first reaction represents the oxidative addition, while the reverse reaction represents the reductive elimination followed by a consecutive migratory carbonyl insertion.

This paper primarily focuses on the first step in Scheme 1, for which the observed pseudo-first-order rate constant ($[CH_3I] \gg [Rh]$) is defined by Eq. (5).

$$(k_{obs})_{OA} = k_{OA}[CH_3I] + k_{RE} \quad (5)$$

The kinetic constants k_{OA} and k_{RE} refer to the rates of the forward (oxidative addition) and reverse (reductive elimination) reactions, respectively. The equilibrium constant for the first step, which defines the thermodynamic feasibility of the reaction to proceed forward, is given by Eq. (6), and are reported in Table 4 together with the rate constants.

$$K_{OA} = \frac{k_{OA}}{k_{RE}} \quad (6)$$

The first step, i.e., oxidative addition and reductive elimination, was conveniently studied using a range of solvents and different CH_3I concentrations at three different temperatures using different kinetic techniques (IR and UV–vis). Analysis of the dependence of the rate of Rh(III)-alkyl formation on $[CH_3I]$, as illustrated in Scheme 1, shows a direct relationship of the pseudo-first-order rate constant on $[CH_3I]$, as illustrated in, e.g. Fig. 11.

These results are consistent with the rate expression shown in Eq. (5), but are also supported by time-resolved IR spectroscopy studied under identical conditions as illustrated in Fig. 9. The conversion to the alkyl species in the case of [Rh(CO)Cl{P(*p*-Tol)$_3$}$_2$] is not complete and much less favoured than in the corresponding [Rh(CO)Cl{As(*p*-Tol)$_3$}$_2$]. In the latter case, conversion toward the Rh(III) alkyl complex is favourable (ν(CO) = 2050 cm^{-1}), but not so for *trans*-[Rh(CO)Cl{P(*p*-Tol)$_3$}$_2$] with the reaction proceeding only to a small extent.

As mentioned above, the crystallographic study showed that *trans*-[Rh(CO)Cl{As(*p*-Tol)$_3$}$_2$] is less sterically crowded than *trans*-[Rh(CO)Cl{P(*p*-Tol)$_3$}$_2$] since introduction of the larger arsine atom increases the 'cavity' in

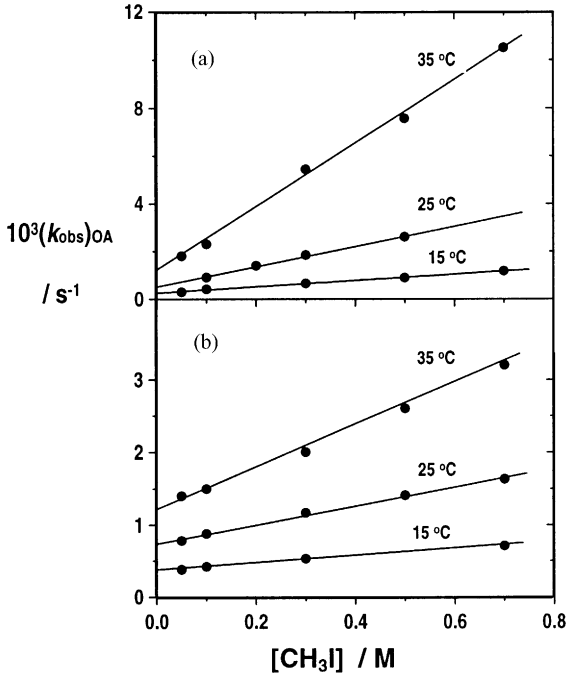

Fig. 11. $[CH_3I]$ and temperature dependence of the pseudo-first-order rate constant for the iodomethane oxidative addition to (a) *trans*-$[Rh(CO)Cl\{As(p\text{-}Tol)_3\}_2]$ and (b) *trans*-$[Rh(CO)Cl\{P(p\text{-}Tol)_3\}_2]$ in acetone (Adapted from Ref. [13], Copyright: The Royal Society of Chemistry, with permission).

the complex from 4.665(1) for the P–P distance to 4.824(1) Å for the As–As. These distances show that the larger As(*p*-Tol)$_3$ complex is less sterically hindered and thus has more space available to accommodate entering moieties, such as, e.g., in iodomethane oxidative addition. This increase in 'cavity' size in the As(*p*-Tol)$_3$ complex is expected to shift the equilibrium more toward the intermediate, resulting in a larger equilibrium constant for the As(*p*-Tol)$_3$ complex than for P(*p*-Tol)$_3$ due to less steric crowding. This is well manifested in the K_{OA} values as presented in Table 5. Of interest is the fact that the first reaction is thermodynamically favoured in both DCM (K_{OA} 9 M^{-1} vs. 1.7 M^{-1}) and acetone (15 M^{-1} vs. 2.3 M^{-1}), respectively, for the As(*p*-Tol)$_3$ complex over the P(*p*-Tol)$_3$ complex. In ethyl acetate and toluene, the equilibrium constants are, strangely enough, quite similar. It is, however, clear from Table 5 that in both ethyl acetate and toluene less accuracy in the determination of the slope (k_{OA}) had been achieved. If the slope is not accurately determined, the corresponding K_{OA} value, which is directly dependent thereupon ($K_{OA} = k_{OA}/k_{RE}$), is similarly less accurately defined.

Eq. (7) illustrates the expression for the observed rate constant for the formation of the Rh(III)-acyl species via migratory carbonyl insertion ($[CH_3I] \gg [Rh]$), as shown in Scheme 1. The constants k_{CI} and k_{-CI}, respectively, represent the forward and reverse steps for the migratory carbonyl insertion reaction, clearly seen in, e.g. Fig. 9.

Table 5
Structural data for Vaska-type complexes of the form *trans*-$[RhCl(CO)(PX_3)_2]$

PX_3	Reference
tris(*p*-Fluorophenyl)phosphine	[77]
tri-*t*-Butylphosphine	[78]
tri-*t*-Butylphosphine	[79]
bis(bis(Trimethylsilyl)methyl)phosphine	[80]
tris(2-Pyridyl)phosphine	[81]
2,6-Difluorophenyl-phenylphosphine	[82]
Triphenylphosphine	[83]
Triphenylphosphine	[84]
Triphenylphosphine	[85]
Triphenylphosphine	[86]
Methyldiphenylphosphine	[87]
Diphenyl(3,3,4,4,5,5,6,6,7,7,8,8,8-tridecafluorooctyl)phosphine	[88]
Triphenylphosphine dichloromethane solvate	[89]
1-Phenyldibenzophosphole dichloromethane solvate	[90]
1-Phenyl-3,4-dimethylphosphole	[90]
Diphenylvinylphosphine	[90]
Dimethylphenylphosphine	[91]
Trifluorosilylethyl(dimethyl)phosphine	[92]
2-Fluorodimethylsilylphenyl(dimethyl)phosphine	[90]
Triphenylphosphine dichloromethane solvate	[48]
Trimethylphosphine	[93]
bis(Dimethylamino)(2,5-dimethyl-1,2,3-diazaphosphol-4-yl) phosphine	[94]
tris(1H,1H,2H,2H-Perfluoro-octyl)phosphine	[95]
tris(3,3,4,4,5,5,6,6,7,7,8,8,8-Tridecafluorooctyl)phosphine	[96]
2-(Diphenylphosphino)pyrimidine	[97]
2,4,6-Triphenylphosphabenzene dichloromethane solvate	[98]
(*o*-Methoxyphenyl)diphenylphosphine	[99]
3-Pyridyldiphenylphosphine	[100]
Triphenylphosphine benzene solvate	[101]
3-(Chloropropyl)dicyclohexylphosphine	[102]
tri-*p*-Tolylphosphine	[20]
Diphenylamino(diphenylphosphino)methane	[103]
bis(Diphenylaminomethyl)phenylphosphine	[103]
o-Chlorophenyl(diphenyl)phosphine dichloromethane solvate	[104]
2-Dimethylphosphino-1,1-di-t-butylethanol	[105]
tri-*t*-Butylphosphine toluene solvate	[79]
tris(*N*-Pyrrolyl)phosphine	[26]
tris(*N*-Pyrrolidinyl)phosphine	[26]
1-Menthyl-3,3,4,4-tetramethyl-2-diphenylphosphinophosphetane dichloromethane solvate	[106]

$$(k_{obs})_{CI} = \frac{(k_{CI}K_{OA}[CH_3I])}{(1 + K_{OA}[CH_3I])} + k_{-CI} \quad (7)$$

In the current study the formation of the final Rh(III)-acyl species, although it has been observed and identified as illustrated above, was not studied in any detail. More detailed investigations on the related $[Rh(L,L'\text{-BID})(CO)(PX_3)_2]$ type complexes are described elsewhere [29].

6.4. Reactivity, activation parameters and solvent effect for iodomethane oxidative addition to rhodium(I) Vaska-type complexes

The relative reactivity of both the oxidative addition and reductive elimination in the *trans*-$[Rh(CO)Cl\{Y(p\text{-}Tol)_3\}_2]$ (Y = As, P) complexes also including $[Rh(CO)Cl(SbPh_3)_2]$

spans about a two order of magnitude range (Table 4). The half-lives for the reaction at ambient temperature and $[CH_3I] = 1$ M, range from a few minutes to hours, and compare well with those observed previously in the $[Rh(CO)Cl(YPh_3)_2]$ (Y = P, As) complexes [10]. The *trans*-$[Rh(CO)Cl\{P(p\text{-}Tol)_3\}_2]$ complex is more reactive in the less polar/coordinating solvents toluene and DCM, but thermodynamically the reaction is less feasible. In acetone and ethyl acetate (both more polar and coordinating), the arsine complex 4–5 more reactive than the P analogue, which suggests an increased solvent contribution in the *trans*-$[Rh(CO)Cl\{As(p\text{-}Tol)_3\}_2]$ complex.

It was illustrated above that significant solvent effects are observed in the pre-equilibrium in the Sb system. However, in the As system, in the oxidative addition reaction, the equilibrium between the rhodium(I) reactant and the rhodium(III) alkyl product is also significantly influenced by the solvent as illustrated in Table 4.

The solvent polarity (as illustrated by the dielectric constant, ε) as a function of relative constant solvent donicity (from the donor number D_N), i.e., for ethyl acetate to acetone and again dichloromethane to toluene, shows an increase of about a one to two order of magnitude in both k_{OA} and K_{OA} for both the *trans*-$[Rh(CO)Cl\{As(p\text{-}Tol)_3\}_2]$ and *trans*-$[Rh(CO)Cl\{P(p\text{-}Tol)_3\}_2]$ complexes. This might be indicative of competition between the CH_3I and good coordinating solvents in the *trans*-$[Rh(CO)Cl\{As(p\text{-}Tol)_3\}_2]$ complex where there is also less steric congestion at the metal centre (see above).

However, k_{RE} for both *trans*-$[Rh(CO)Cl\{P(p\text{-}Tol)_3\}_2]$ and *trans*-$[Rh(CO)Cl\{As(p\text{-}Tol)_3\}_2]$ shows a small decrease in reactivity with an increase in polarity, i.e., in the case of the P-complex a decrease of only ca. 1.2 × is observed from ethyl acetate to acetone, and 1.5 × from toluene to dichloromethane, respectively. In the case of the *trans*-$[Rh(CO)Cl\{As(p\text{-}Tol)_3\}_2]$ complex, a one order of magnitude increase is observed. This indicates that the reductive elimination is inhibited by solvent polarity, but that oxidative addition seems to be favoured.

The different steps in the above-mentioned reaction sequence are thus differently influenced in the two complexes, but the net effect on the stability constant K_{OA} is the same. Also it cannot be excluded that the larger intercepts in the case of ethyl acetate in general (Table 4) might incorporate contributions from a possible concurrent route via a solvent pathway as well as the reductive elimination process.

Both the *trans*-$[Rh(CO)Cl(SbPh_3)_2]$ and *trans*-$[Rh(CO)Cl\{As(p\text{-}Tol)_3\}_2]$ complexes show comparable reactivity, which suggests similar electron density on the Rh-centre in both.

Upon examination of the activation parameters as summarised in Table 4, it is clear that these are characterised by positive values of $\Delta H^{\neq} k_{OA}$ and negative values of $\Delta S^{\neq} k_{OA}$, which indicate that bond formation plays an important role in forming the transition state. This was already pointed out in previous work where it was shown that the oxidative addition reaction proceeds via an associative mechanism [76].

Since reductive elimination is the opposite of oxidative addition, it is the expected to proceed via a more dissociative pathway, possibly showing positive value of $\Delta S^{\neq}_{RE}$. This was however not observed, although it is of interest to note that in the *trans*-$[Rh(CO)Cl\{As(p\text{-}Tol)_3\}_2]$ complex

Table 6
Dinuclear complexes containing rhodium(I) Vaska-type fragments

Compound Name	Reference
Dicarbonyl-dichloro-bis(μ2-2,6-bis(diphenylphosphinomethyl)benzene)-di-rhodium	[107]
bis(μ2-2,6-bis(Diphenylphosphino)-pyridine-P,P′)-chloro-dicarbonyl-methanol-di-rhodium hexafluorophosphate dichloromethane solvate	[108]
Chlorocarbonyl-(sulfur dioxide)-bis(triphenylphosphine)rhodium	[109]
Dicarbonyl-dichloro-bis(μ2-bis((diphenylphosphino)methyl)-phenylarsine)-di-rhodium dichloromethane solvate	[110]
Dicarbonyl-dichloro-bis(μ2-bis((diphenylphosphino)methyl)phenylarsine-P,P′)-di-rhodium dichloromethane solvate	[111]
bis((μ2-bis(Diphenylphosphino)-methane)-chloro-carbonyl-rhodium)	[112]
Dicarbonyl-trichloro-bis(μ2-bis((diphenylphosphino)methyl)phenylarsine-P,P′)-silver-di-rhodium dichloromethane solvate	[107]
Carbonyl-chloro-bis(tris(2-*t*-butylphenyl)phosphito)rhodium	[113]
trans-Carbonyl-chloro-bis(perfluorohexylethoxy(diphenyl)phosphine)rhodium(i)	[114]
(*N*,*N*′-bis(2-(Diphenylphosphino)phenyl)propane-1,3-diamine)-carbonyl-chloro-rhodium(i)	[115]
(*N*,*N*′-bis(2-(Diphenylphosphino)phenyl)propane-1,3-diamine)-carbonyl-chloro-rhodium(i)	[116]
trans-Carbonyl-chloro-((*S*,*S*)-2,2′-bis((*R*)-1-(di-*n*-butylphosphino)ethyl)-1,1′-biferrocene)rhodium(i)	[117]
trans-Carbonyl-chloro-((*S*,*S*)-2,2-bis((*R*)-1-(di-*n*-butylphosphino)ethyl)-1,1′-biferrocene)rhodium	[118]
Di-μ-(1,5-bis(diphenylphosphino)-3-oxapentane)-bis(*trans*-carbonyl-chloro-rhodium(i))methylene dichloride solvate	[119]
Carbonyl-chloro-(2,11-bis(diphenylphosphinomethyl)benzo(c)phenanthrene)rhodium benzonitrile solvate	[120]
Carbonyl-chloro-(1,6-bis(((1-menth-3′-yl)-2,2,3,3-tetramethylphosphetan-4-yl)dimethylsilyl)hexane)rhodium hexane solvate	[121]
bis((μ2-bis(bis(Benzothiazol-2-yl)phosphino)methane-P,P′)-carbonyl-chloro-rhodium)tetrahydrofuran solvate	[122]
trans-Carbonyl-chloro-bis(1,3,5-triethylbiuret phenoxyphosphorus diamide)rhodium benzene solvate	[123]
trans-Carbonyl-chloro-bis(1,3,5-triphenylbiuret phenoxyphosphorus diamide)rhodium	[123]
bis((μ2-1,4-bis(2-Diphenylphosphinoethoxy)benzene)-carbonyl-chloro-rhodium(i)) unknown solvate	[124]
tetrakis(μ2-η5-(2-(Diphenylphosphino)ethyl)cyclopentadienyl)-dicarbonyl-hexachloro-di-rhodium(i)-di-titanium	[125]
tetrakis(μ2-η5-((Diphenylphosphino)methyl)cyclopentadienyl)-dicarbonyl-hexachloro-di-rhodium(i)-di-titanium dichloromethane solvate	[125]
Carbonyl-chloro-((*S*,*S*)-(*R*,*R*)-2,2′′-bis(1-(bis(2-furyl)phosphino)ethyl)-1,1′′-biferrocene)rhodium dichloromethane solvate	[126]

Table 7
Iodo complexes containing rhodium(I) and rhodium(III) Vaska-type fragments

Compound name	Reference
trans-Carbonyliodobis(triphenylphosphine)rhodium(I)	[42]
Carbonyliodotris(1-methyl-1-azonia-3,5-diaza-7-phospha-adamantane)rhodium(I) triiodide tetrahydrate	[49]
Carbonylchloroiodo(iodomethyl)-bis(triethylphosphine)-rhodium(III)	[127]
Carbonyldiiodomethyl-bis(triethylphosphine)rhodium(III)	[128]
Carbonyldiiodomethyl-bis(triethylphosphine)rhodium(III)	[129]
trans-Carbonyl-tris(iodo)-bis(triphenylphosphine)rhodium(III)	[130]

smaller negative values for both $\Delta S^{\neq} k_{OA}$ and $\Delta S^{\neq} k_{RE}$ have been obtained. Less ordered transition states wherein significant solvent interaction exists are therefore probable, but additional research is needed to address these aspects.

As mentioned above, although the formation of the final Rh(III)-acyl species was observed (see, e.g. Fig. 9), its formation was not studied in any detail. Nevertheless, it is of interest to note that Eq. (7) predicts that at low [CH_3I], the rate of formation of the acyl species is first order in [CH_3I], and directly proportional to the stability constant K_{OA}. In the case of the *trans*-[Rh(CO)Cl{P(*p*-Tol)$_3$}$_2$] complex, the effective rate of formation of the acyl species is generally decreased (by at least a factor of 5), since the conversion of the P(*p*-Tol)$_3$ complex to the intermediate [Rh(CO)Cl(CH_3)I{P(*p*-Tol)$_3$}$_2$] species, is thermodynamically less feasible.

7. Concluding remarks

Different aspects of the rhodium(I) Vaska-type complexes have been illustrated, particularly that they are still excellent model complexes to study basic effects such as the solid-state structures to be incorporated in the broader picture of the reaction mechanism to explain solution effects. Similarly, these sterically congested systems enabled different solvent effects to be studied and are good models for theoretical calculations. However, additional research is still required to aid in understanding solution behaviour of these systems.

Acknowledgements

Part of this material is based on work supported by the South African National Research Foundation under Grant number (GUN 2053397). Any opinion, findings and conclusions or recommendations expressed in this material are those of the authors and do not necessarily reflect the views of the NRF. Financial assistance from the Swedish International Development and Co-operation Agency (SIDA) and the Research Fund of the RAU is also gratefully acknowledged. Lund University (Prof. Åke Oskarsson) and the University of Witwatersrand (Prof. D. Levendis) are thanked for the use of their diffractometers for some data collections reported in this paper.

Appendix A

Representative structures of rhodium(I) Vaska-type complexes (*trans*-[Rh(CO)Cl(PX$_3$)$_2$]) are given in Table 5. Dinuclear complexes containing rhodium(I) Vaska-type fragments are given in Table 6. Iodo complexes containing rhodium(I) and rhodium(III) Vaska-type fragments are given in Table 7.

References

[1] M. Angoletta, Gazz. Chim. Ital. 89 (1959) 2359.
[2] L. Vaska, J.W. DiLuzio, J. Am. Chem. Soc. 83 (1961) 2784.
[3] L. Vallarino, J. Chem. Soc. (1957) 2287.
[4] J. Chatt, B. Shaw, Chem. Ind. (1961) 290.
[5] H.A. Zahalka, H. Alper, Organometallics 5 (1986) 2597 For example
[6] M. Selke, W.L. Karney, S.I. Kahn, C.S. Foote, Inorg. Chem. 34 (1995) 5715, (and references within) For example
[7] J. Chatt, L.A. Duncanson, J. Chem. Soc. (1953) 2939.
[8] M.C. Baird, G. Wilkinson, J. Chem. Soc. Chem. Commun. (1966) 267.
[9] M.J. Mays, G. Wilkinson, J. Chem. Soc. (1965) 6629.
[10] I.C. Douek, G. Wilkinson, J. Chem. Soc. A (1969) 2604.
[11] A. Roodt, S. Otto, J.G. Leipoldt, Acta Crystallogr. C 51 (1996) 1105.
[12] S. Otto, A. Roodt, Acta Crystallogr. C 53 (1997) 280.
[13] S. Otto, S.N. Mzamane, A. Roodt, in: G.J. Leigh, N. Winterton (Eds.), Legacy of J. Chatt, Royal Society of Chemistry, Oxford, UK, 2002, pp. 328–340.
[14] S. Otto, A. Roodt, Inorg. Chim. Acta (2002) 199.
[15] S. Otto, A. Roodt, Acta Crystallogr. C 53 (1997) 1414.
[16] S. Otto, A. Roodt, J.J.C. Erasmus, J.C. Swarts, Polyhedron 17 (1998) 2447.
[17] S. Otto, A. Roodt, J. Smith, Inorg. Chim. Acta 303 (2000) 295.
[18] G. Steyl, S. Otto, A. Roodt, Acta Crystallogr. E 57 (2001) m352.
[19] (a) F.H. Allen, O. Kennard, Chem. Des. Autom. News 8 (1993) 31; (b) Cambridge Structural Database, Cambridge Crystallographic Data Centre, Cambridge, UK, 2001.
[20] S. Otto, S.N. Mzamane, A. Roodt, Acta Crystallogr. C 55 (1999) 67.
[21] G.O. Spessard, G.L. Miessler, Organometallic Chemistry, Prentice-Hall, Englewood Cliffs, NJ, 1997.
[22] W.A. Herrmann, in: B. Cornils, W.A. Herrmann (Eds.), Applied Homogeneous Catalysis with Organometallic Compounds, VCH, Weinheim, 1995.
[23] C.A. Tolman, Chem. Rev. 77 (1977) 313.
[24] M.R. Wilson, A. Prock, W.P. Giering, A.L. Fernandez, C.M. Haar, S.P. Nolan, B.M. Foxman, Organometallics 21 (2002) 2758 (and references within).
[25] D.W. Allen, B.F. Taylor, J. Chem. Soc. Dalton Trans. (1982) 51.
[26] K.G. Moloy, J.L. Petersen, J. Am. Chem. Soc. 117 (1995) 7696.
[27] Typical synthesis, e.g., *trans*-[Rh(CO)Cl{P(*p*-Tol)$_3$}$_2$] and *trans*-[Rh(CO)Cl{As(*p*-Tol)$_3$}$_2$]: [Rh(μ-Cl)(CO)$_2$]$_2$ (25 mg, 0.064 mmol) was dissolved in acetone (3 cm^3) and the appropriate ligand (0.28 mmol) also dissolved in acetone (4 cm^3) was added. Effervescence can be observed as CO is liberated. Crystals suitable for X-ray analysis can be obtained by slow evaporation of these solutions.

[28] D.D. Perrin, W.L.F. Armarego, Purification of Laboratory Chemicals, 3rd ed, Pergamon Press, Oxford, 1988.

[29] A. Roodt, G.J.J. Steyn, in: S.G. Pandalai (Ed.), Res. Research Dev. Inorg. Chem., vol. 2, Transworld Research Network, Trivandrum, 2000, pp. 1–23 (Chapter 1).

[30] SCIENTIST for Windows, program for least-squares parameter estimation, version 4.00.950, MicroMath Scientific Software, UT, USA, 1990.

[31] G.J.J. Steyn, A. Roodt, A. Poletaeva, Y. Varshavsky, J. Organomet. Chem. 536/537 (1997) 797.

[32] Three-dimensional intensity data collected on a Bruker SMART CCD diffractometer at 293(2) K; Mo–K_α radiation (0.71073 Å); reflections corrected for Lorentz and polarization effects and absorption corrections applied using SADABS; structures solved by direct method and successive Fourier synthesis (SHELXS-97 and SHELXL-97); hydrogen atoms placed in calculated positions with fixed isotropic thermal parameters; $R = \Sigma\Delta F/\Sigma F_o$; $R_w = \Sigma w(F_o^2 - F_c^2)^2/\Sigma[w(F_o^2)^2]^{1/2}$.

[33] G.M. Sheldrick, SADABS, program for absorption corrections to area detector data, University of Göttingen, Germany, 1999.

[34] G.M. Sheldrick, SHELXS-97, program for solving crystal structures, University of Göttingen, Germany, 1997.

[35] G.M. Sheldrick, SHELXL-97, program for refining crystal structures, University of Göttingen, Germany, 1997.

[36] K. Brandenburg, M. Berndt, DIAMOND, Version 2.1c, Crystal Impact GbR, Bonn, Germany, 1999.

[37] J.W. Akitt, B.E. Mann, NMR and Chemistry, Stanley Thornes Ltd, Cheltenham, UK, 2000, p. 4.

[38] S. Otto, Acta Crystallogr. C 57 (2001) 793.

[39] G. Ferguson, P.J. Roberts, E.C. Alyea, M. Khan, Inorg Chem. 17 (1978) 2965.

[40] N. Grimmer, N.J. Coville, South Afr. J. Chem. 54 (2001) 50.

[41] (a) P.B. Dias, M.E. Minas de Pidade, J.A.M. Simoes, Coord. Chem. Rev. 135/136 (1994) 737;
(b) A.J. Poë, Organometallics (2002) 281.

[42] S.S. Basson, J.G. Leipoldt, A. Roodt, Acta Crystallogr. Sect. C (Cr. Str. Comm.) 46 (1990) 142.

[43] S. Otto, A. Roodt, Inorg. Chim. Acta., in press

[44] G. Kemp, W. Purcell, A. Roodt, K. Koch, J. Chem. Soc. Dalton Trans. (1997) 4481.

[45] S. Otto, A. Roodt, Acta Crystallogr. C 52 (1996) 1636.

[46] T.S. Janik, M.R. Churchill, R.F. See, S.L. Randall, J.M. McFarland, J.D. Atwood, Acta Crystallogr. Sect. C 48 (1992) 1493.

[47] S. Otto, Ph.D. Thesis, Free State University, Bloemfontein, South Africa, 1999.

[48] K.R. Dunbar, S.C. Haefner, Inorg. Chem. 31 (1992) 3676.

[49] F.P. Pruchnik, P. Smolenski, E. Galdecka, Z. Galdecki, New J. Chem. 22 (1998) 1395.

[50] S. Otto, A. Roodt, Acta. Crystallogr. C 58 (2002) m565.

[51] G.J. Lamprecht, C.P. Van Biljon, J.G. Leipoldt, Inorg. Chim. Acta 119 (1986) L1.

[52] M.R. Churchill, J.C. Fettinger, L.A. Buttrey, M.D. Barkan, J.S. Thompson, J. Organomet. Chem. 340 (1988) 257.

[53] M. Selke, C.S. Foote, W.L. Karney, Inorg. Chem. 32 (1993) 5425.

[54] M.R. Churchill, J.C. Fettinger, B.J. Rappoli, J.D. Atwood, Acta Crystallogr. C 43 (1987) 1697.

[55] E. Kuwabara, R. Bau, Acta Crystallogr. C 50 (1994) 1409.

[56] A.N. Sobolev, I.P. Romm, V.K. Belsky, E.N. Guryanova, J. Organomet. Chem. 179 (1979) 153.

[57] J. Liedtke, S. Loss, G. Alcaraz, V. Gramlich, H. Grützmacher, Angew. Chim. Int. Ed. 38 (1999) 1623.

[58] J. Liedtke, H. Ruegger, S. Loss, H. Grützmacher, Angew. Chim. Int. Ed. 39 (2000) 2478.

[59] G. Kemp, A. Roodt, W. Purcell, Rhodium Express 12 (1995) 21.

[60] W. Hieber, H. Heusinger, O. Vohler, Chem. Ber. 90 (1957) 2425.

[61] M.A. Jennings, A. Wojcicki, Inorg. Chem. 6 (1967) 1854.

[62] W. Hieber, V. Frey, Chem. Ber. 99 (1966) 2614.

[63] R. Ugo, F. Bonati, S. Cenini, Inorg. Chim. Acta 3 (1969) 220.

[64] L. Vallarino, Personal communication.

[65] V. Gutmann, Coord. Chem. Rev. 18 (1976) 225.

[66] M. Sandstrom, I. Persson, P. Persson, Acta Chim. Scand. 44 (1990) 653.

[67] J. Rydberg, in: J. Rydberg, C. Musikas, G. Choppin (Eds.), Principles and Practices of Solvent Extraction, Marcel Dekker, New York, 1992, p. 23.

[68] G.J.J. Steyn, A. Roodt, J.G. Leipoldt, Inorg. Chem. 31 (1992) 3477.

[69] G. Steyl, M.Sc. Thesis, University of the Free State, Bloemfontein, South Africa, 1999.

[70] Empirical formula: $C_{44}H_{32}Br_3O_3P_2Rh$; FW: 1013.3; crystal system: monoclinic; space group: $P2/n$; $a = 11.945(2)$ Å; $b = 24.271(5)$ Å; $c = 14.006(3)$ Å; $\beta = 97.69(3)^\circ$; $V = 3949.6(14)$ Å^3; $Z = 4$; $D_c = 1.704$ g cm^{-3}; $\mu = 3.589$ mm^{-1}; $T_{max}/T_{min} = 0.505/0.241$; $F(0\,0\,0) = 2000$; crystal size: $0.13 \times 0.13 \times 0.21$ mm^3; θ_{limit}: 5.10–30.51°; index ranges: $-16 \le h \le 17$; $-32 \le k \le 33$; $-20 \le l \le 17$; collected reflections: 38 851; independent reflections: 11 824; observed reflections: $I > 2(\sigma)I$: 7161; data/restr./param. 11 824/0/479; Goo$F$: 0.745; R/R_w ($I > 4(\sigma)I$): 0.0523; 0.0976; R/R_w (all data) 0.2485, 0.1307; $\Delta\rho_{max}$, $\Delta\rho_{min}$: 0.750, −1.249 e Å^{-3}. Selected bond distances and angles: Rh–C(1), 1.831(8) Å; Rh–O(2), 2.161(4) Å; Rh–P(1), 2.3337(17) Å; Rh–P(2), 2.3367(17) Å; Rh–O(3), 2.485(4) Å; C(1)–O(1), 1.056(7) Å; P(1)–Rh–P(2), 179.02(6)°; C(1)–Rh–O(2), 161.5(2)°; C(1)–Rh–P(2), 90.99(19)°; O(2)–Rh–O(3), 66.66(15)°; O(1)–C(1)–Rh, 178.1(6)°. Empirical formula: $C_{44}H_{32}Br_3O_3As_2Rh$; FW: 1101.2; crystal system: monoclinic; space group: $P2/n$; $a = 11.945(2)$ Å; $b = 24.271(5)$ Å; $c = 14.006(3)$ Å; $\beta = 97.60(3)^\circ$; $V = 4024.9(14)$ Å^3; $Z = 4$; $D_c = 1.817$ g cm^{-3}; $\mu = 5.074$ mm^{-1}; $T_{max}/T_{min} = 0.505/0.241$; $F(0\,0\,0) = 2144$; crystal size $= 0.13 \times 0.13 \times 0.24$ mm^3; $\theta_{limit} = 1.68$–31.86°; index ranges: $-13 \le h \le 17$; $-34 \le k \le 34$; $-20 \le l \le 19$; collected reflections: 41 173; independent reflections: 12 548; observed reflections, $I > 2(\sigma)I$: 6085; data/restr./param.: 12 548/0/478; Goo$F$, 0.789; R/R_w ($I > 4(\sigma)I$): 0.0581, 0.1158; R/R_w (all data) 0.2570, 0.1514; $\Delta\rho_{max}$, $\Delta\rho_{min}$: 1.089, −1.170 e Å^{-3}. Selected bond distances and angles: Rh–C(1), 1.829(11) Å; Rh–O(2), 2.166(5) Å; Rh–As(2), 2.4055(10) Å; Rh–As(1), 2.4117(10) Å; Rh–O(3), 2.464(6) Å; O(1)–C(1), 1.075(10) Å; As(2)–Rh–As(1), 179.25(4)°; C(1)–Rh–O(2), 161.1(3)°; C(1)–Rh–As(2), 90.5(3)°; O(2)–Rh–O(3), 66.76(19)°; O(1)–C(1)–Rh, 178.0(9)°.

[71] S.S. Basson, J.G. Leipoldt, A. Roodt, J.A. Venter, Inorg. Chim. Acta 118 (1986) L45.

[72] M. Cano, J.V. Heras, M.A. Lobo, E Pinilla, Polyhedron 11 (1992) 2679.

[73] K. van Aswegen, J.G. Leipoldt, I.M. Potgieter, G.J. Lamprecht, A. Roodt, G. van Zyl, Transition Met. Chem. 16 (1991) 369.

[74] L.J. Damoense, Ph.D. Thesis, Free State University, Bloemfontein, South Africa, 2000.

[75] A. Kayan, J.C. Gallucci, A. Wojcicki, Inorg. Chem. Commun. 1 (1998) 446.

[76] J.G. Leipoldt, R. van Eldik, J.A. Venter, Inorg. Chem. 30 (1991) 2207 See, for example

[77] A. Monge, E. Gutierrez-Puebla, J.V. Heras, E. Pinilla, Acta Crystallogr. Sect. C (Cr. Str. Comm.) 39 (1983) 446.

[78] H. Schumann, M. Heisler, J. Pickardt, Chem. Ber. 110 (1977) 1020.

[79] R.L. Harlow, S.A. Westcott, D.L. Thorn, R.T. Baker, Inorg. Chem. 31 (1992) 323.

[80] B.D. Murray, H. Hope, J. Hvoslef, P.P. Power, Organometallics 3 (1984) 657.

[81] K. Wajda, F. Pruchnik, T. Lis, Inorg. Chim. Acta 40 (1980) 207.

[82] C. Corcoran, J. Fawcett, S. Friedrichs, J.H. Holloway, E.G. Hope, D.R. Russell, G.C. Saunders, A.M. Stuart, J. Chem. Soc. Dalton Trans. (2000) 161.

[83] A. Del Pra, G. Zanotti, P. Segala, Cryst. Struct. Commun. 8 (1979) 959.

[84] A. Ceriotti, G. Ciani, A. Sironi, J. Organomet. Chem. 247 (1983) 345.
[85] A.L. Rheingold, S.J. Geib, Acta Crystallogr. Sect. C (Cr. Str. Comm.) 43 (1987) 784.
[86] Y.-J. Chen, J.-C. Wang, Y. Wang, Acta Crystallogr. Sect. C (Cr. Str. Comm.) 47 (1991) 2441.
[87] F. Dahan, R. Choukroun, Acta Crystallogr. Sect. C (Cr. Str. Comm.) 41 (1985) 704.
[88] D.C. Smith Jr., E.D. Stevens, S.P. Nolan, Inorg. Chem. 38 (1999) 5277.
[89] P.A. Chaloner, C. Claver, P.B. Hitchcock, A.M. Masdeu, A. Ruiz, Acta Crystallogr. Sect. C (Cr. Str. Comm.) 47 (1991) 1307.
[90] J.M. Kessler, J.H. Nelson, J.S. Frye, A. DeCian, J. Fischer, Inorg. Chem. 32 (1993) 1048.
[91] H. Schumann, S. Jurgis, M. Eisen, J. Blum, Inorg. Chim. Acta 172 (1990) 191.
[92] J. Grobe, R. Martin, G. Huttner, L. Zolnai, Z. Anorg. Allg. Chem. 607 (1992) 79.
[93] S.E. Boyd, L.D. Field, T.W. Hambley, M.G. Partridge, Organometallics 12 (1993) 1720.
[94] M.D. Mikoluk, R. McDonald, R.G. Cavell, Organometallics 18 (1999) 3306.
[95] J. Fawcett, E.G. Hope, R.D.W. Kemmitt, D.R. Paige, D.R. Russell, A.M. Stuart, D.J. Cole-Hamilton, M.J. Payne, Chem. Commun. (1997) 1127.
[96] M.-A. Guillevic, C. Rocaboy, A.M. Arif, I.T. Horvath, J.A. Gladysz, Organometallics 17 (1998) 707.
[97] S.-L. Li, Z.-Z. Zhang, B.-M. Wu, T.C.W. Mak, Inorg. Chim. Acta 255 (1997) 239.
[98] B. Breit, R. Winde, T. Mackewitz, R. Paciello, K. Harms, Chem. Eur. J. 7 (2001) 3106.
[99] P. Suomalainen, S. Jaaskelainen, M. Haukka, R.H. Laitinen, J. Pursiainen, T.A. Pakkanen, Eur. J. Inorg. Chem. (2000) 2607.
[100] R.H. Laitinen, J. Soininen, P. Suomalainen, T.A. Pakkanen, M. Ahlgren, J. Pursiainen, Acta Chem. Scand. 53 (1999) 335.
[101] P. Sharma, A. Cabrera, R. Le Lagadec, R.L. Manzo, G. Espinosa, M. Sharma, J.L. Arias, Acta Cienc. Indica, Ser. Chem. 24 (1998) 137.
[102] E. Lindner, R. Fawzi, H.A. Mayer, W. Hiller, Private Communication, 1992.
[103] A.L. Balch, M.M. Olmstead, S.P. Rowley, Inorg. Chim. Acta 168 (1990) 255.
[104] P. Lahuerta, J. Latorre, R. Martinez-Manez, F. Sanz, J. Organomet. Chem. 356 (1988) 355.
[105] P.B. Hitchcock, M.F. Lappert, I.A. MacKinnon, Chem. Commun. (1993) 1015.
[106] A. Marinetti, C. Le Menn, L. Ricard, Organometallics 14 (1995) 4983.
[107] J.R. Dilworth, Y. Zheng, D.V. Griffiths, J. Chem. Soc. Dalton Trans. (1999) 1877.
[108] F.E. Wood, J. Hvoslef, A.L. Balch, J. Am. Chem. Soc. 105 (1983) 6986.
[109] K.W. Muir, J.A. Ibers, Inorg. Chem. 8 (1969) 1921.
[110] A.L. Balch, L.A. Fossett, M.M. Olmstead, D.E. Oram, P.E. Reedy Jr., J. Am. Chem. Soc. 107 (1985) 5272.
[111] A.L. Balch, M. Ghedini, D.E. Oram, P.E. Reedy Jr., Inorg. Chem. 26 (1987) 1223.
[112] M. Cowie, S.K. Dwight, Inorg. Chem. 19 (1980) 2500.
[113] E. Fernandez, A. Ruiz, C. Claver, S. Castillon, A. Polo, J.F. Piniella, A. Alvarez-Larena, Organometallics 17 (1998) 2857.
[114] C.M. Haar, J. Huang, S.P. Nolan, J.L. Petersen, Organometallics 17 (1998) 5018.
[115] M.K. Cooper, P.A. Duckworth, T.W. Hambley, G.J. Organ, K. Henrick, M. McPartlin, A. Parekh, J. Chem. Soc. Dalton Trans. (1989) 1067.
[116] R.E. Marsh, Acta Crystallogr. Sect. B(Str. Sci.) 53 (1997) 317.
[117] M. Sawamura, R. Kuwano, Y. Ito, Angew. Chem. Int. Ed. Engl. 33 (1994) 111.
[118] R. Kuwano, M. Sawamura, S. Okuda, T. Asai, Y. Ito, M. Redon, A. Krief, Bull. Chem. Soc. Jpn. 70 (1997) 2807.
[119] N.W. Alcock, J.M. Brown, J.C. Jeffrey, J. Chem. Soc. Dalton Trans. (1977) 888.
[120] F. Bachechi, L. Zambonelli, L.M. Venanzi, Helv. Chim. Acta 60 (1977) 2815.
[121] A. Marinetti, V. Kruger, C. Le Menn, L. Ricard, J. Organomet. Chem. 522 (1996) 223.
[122] M.F.M. Al-Dulaymmi, D.L. Hughes, R.L. Richards, J. Organomet. Chem. 424 (1992) 79.
[123] S.C. van der Slot, P.C.J. Kamer, P.W.N.M. van Leeuwen, J. Fraanje, K. Goubitz, M. Lutz, A.L. Spek, Organometallics 19 (2000) 2504.
[124] F.M. Dixon, A.H. Eisenberg, J.R. Farrell, C.A. Mirkin, L.M. Liable-Sands, A.L. Rheingold, Inorg. Chem. 39 (2000) 3432.
[125] T.W. Graham, A. Llamazares, R. McDonald, M. Cowie, Organometallics 18 (1999) 3502.
[126] M. Sawamura, H. Hamashima, M. Sugawara, R. Kuwano, Y. Ito, Organometallics 14 (1995) 4549.
[127] R.C. Gash, D.J. Cole-Hamilton, R. Whyman, J.C. Barnes, M.C. Simpson, J. Chem. Soc. Dalton Trans. (1994) 1963.
[128] J. Rankin, A.D. Poole, A.C. Benyei, D.J. Cole-Hamilton, Chem. Commun. (1997) 1835.
[129] J. Rankin, A.C. Benyei, A.D. Poole, D.J. Cole-Hamilton, J. Chem. Soc. Dalton Trans. (1999) 3771.
[130] J.R. Dilworth, D. Morales, Y. Zheng, J. Chem. Soc. Dalton Trans. (2000) 3007.